



Versatile ferrous oxidation–xylenol orange assay for high-throughput screening of lipoxygenase activity

Ruth Chrisnasari^{1,2,3} · Tom A. Ewing² · Roelant Hilgers¹ · Willem J. H. van Berkel¹ · Jean-Paul Vincken¹ · Marie Hennebelle¹

Received: 23 November 2023 / Revised: 2 February 2024 / Accepted: 28 February 2024
© The Author(s) 2024

Abstract

Lipoxygenases (LOXs) catalyze dioxygenation of polyunsaturated fatty acids (PUFAs) into fatty acid hydroperoxides (FAHPs), which can be further transformed into a number of value-added compounds. LOXs have garnered interest as biocatalysts for various industrial applications. Therefore, a high-throughput LOX activity assay is essential to evaluate their performance under different conditions. This study aimed to enhance the suitability of the ferrous-oxidized xylenol orange (FOX) assay for screening LOX activity across a wide pH range with different PUFAs. The narrow linear detection range of the standard FOX assay restricts its utility in screening LOX activity. To address this, the concentration of perchloric acid in the xylenol orange reagent was adjusted. The modified assay exhibited a fivefold expansion in the linear detection range for hydroperoxides and accommodated samples with pH values ranging from 3 to 10. The assay could quantify various hydroperoxide species, indicating its applicability in assessing LOX substrate preferences. Due to sensitivity to pH, buffer types, and hydroperoxide species, the assay required calibration using the respective standard compound diluted in the same buffer as the measured sample. The use of correction factors is suggested when financial constraints limit the use of FAHP standard compounds in routine LOX substrate preference analysis. FAHP quantification by the modified FOX assay aligned well with results obtained using the commonly used conjugated diene method, while offering a quicker and broader sample pH range assessment. Thus, the modified FOX assay can be used as a reliable high-throughput screening method for determining LOX activity.

Key points

- *Modifying perchloric acid level in FOX reagent expands its linear detection range*
- *The modified FOX assay is applicable for screening LOX activity in a wide pH range*
- *The modified FOX assay effectively assesses substrate specificity of LOX*

Keywords Fatty acids · FOX assay · High-throughput screening · Hydroperoxides · Lipoxygenase

Introduction

Lipoxygenases (LOXs; EC 1.13.11.x) are non-heme iron- (or in some cases manganese-) dependent enzymes that catalyze dioxygenation of polyunsaturated fatty acids (PUFAs) containing a (1Z,4Z)-pentadiene structural unit, leading to the formation of fatty acid hydroperoxides (FAHPs) containing a (1Z,3E)-conjugated diene pattern. LOX catalyzes the dioxygenation of fatty acids in four distinct steps (Fig. 1): (1) Ferric iron (Fe^{3+}) cofactor initiates the reaction by abstracting a hydrogen atom at the center of the pentadiene structure of the substrate (Lehnert and Solomon 2003), the unpaired electron is transferred to the ferric iron thereby reducing it to the ferrous form (Fe^{2+}), and the proton is transferred to

✉ Tom A. Ewing
tom.ewing@wur.nl

✉ Marie Hennebelle
marie.hennebelle@wur.nl

¹ Laboratory of Food Chemistry, Wageningen University & Research, Bornse Weilanden 9, 6708 WG Wageningen, The Netherlands

² Wageningen Food & Biobased Research, Wageningen University & Research, Bornse Weilanden 9, 6708 WG Wageningen, The Netherlands

³ Faculty of Biotechnology, University of Surabaya (UBAYA), Surabaya 60293, Indonesia

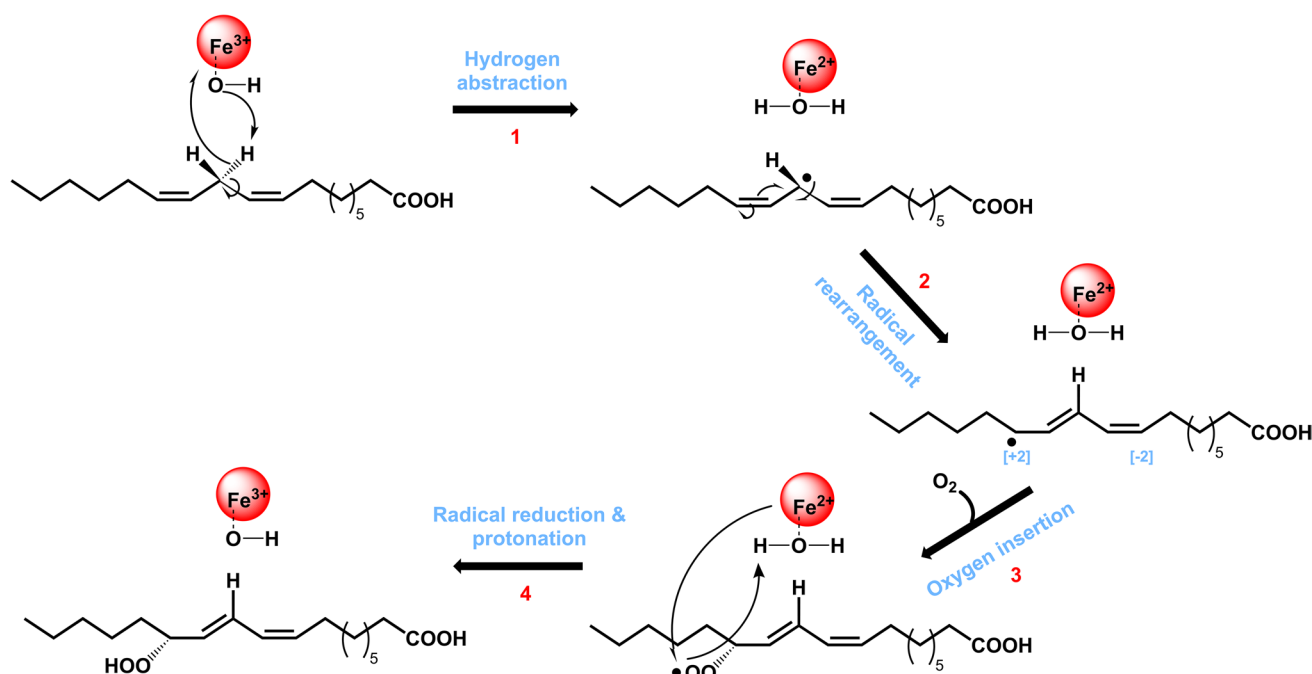


Fig. 1 Reaction mechanism of lipoxygenase (LOX). LOX catalyzes the oxygenation of fatty acids through four reaction steps: hydrogen abstraction, radical rearrangement, oxygen insertion, and radical

reduction-protonation. The figure is adopted from Chrisnasari et al. (2022) with slight modification

the hydroxide ligand that is coordinated to the iron, yielding ferrous iron, water, and a lipid alkyl radical. (2) The unpaired electron generated in the substrate undergoes rearrangement to either the $[\pm 2]$ position relative to the abstracted hydrogen. (3) A dioxygen molecule is introduced leading to the formation of a fatty acid peroxy radical ($\text{ROO}\cdot$). (4) The fatty acid peroxy radical is then reduced by an electron from the ferrous iron (Fe^{2+}) and protonated, resulting in the formation of FAHP (Hamberg and Samuelsson 1967; Egmond et al. 1972; Hamberg et al. 1998; Lehnert and Solomon 2003). FAHPs produced by LOXs can be transformed to numerous value-added compounds, e.g., hydroxy fatty acids, aldehydes, and alcohols (Gigot et al. 2010; Song et al. 2013). These compounds are of interest to the chemical and food industries because they can be used as precursors for the production of biopolymers, surfactants, and flavor compounds (Gigot et al. 2010; Mutlu and Meier 2010; Liu et al. 2012; Song et al. 2013; Hu et al. 2014).

The industrial potential of LOX has led to the exploration of this enzyme from various sources. Among these sources, microbial LOXs have gained increasing attention in recent years for their ability to act on a wide range of PUFAs (Banthiya et al. 2016; Newie et al. 2016; An et al. 2018; Goloshchapova et al. 2018; Qi et al. 2020; Chrisnasari et al. 2022; Kim et al. 2022) and some of them were optimally active at extreme pH values (Qian et al. 2017; Goloshchapova et al.

2018). These advantages stimulate their exploitation as an industrial biocatalyst in a wide range of applications. To facilitate the biocatalytic exploitation of microbial LOXs, it is essential to establish a robust and reliable high-throughput screening method for LOX activity. Due to the wide range of pH values in which microbial LOXs have shown to be active and their ability to convert a range of different PUFAs, this method should enable the rapid assessment of their activity toward various PUFA substrates at different pH values.

LOX activity can be measured either directly or indirectly (Table 1). Direct methods involve measuring either the formation of LOX products (i.e., FAHPs) or the decrease of substrates or co-substrates (i.e., fatty acids or O_2), whereas indirect methods monitor the reaction between LOX products and other compounds. Direct measurement of LOX activity can be done by following the formation of FAHPs using spectrophotometric analysis. For example, a commonly used method is to measure the formation of conjugated diene moieties at a wavelength of 233–235 nm (Corongiu and Milia 1983). However, this method is limited in terms of buffer compatibility, as many chemicals used for buffer preparation (e.g., citric acid (Krukowski et al. 2017), glycine (Gao and Zhang 2018), potassium hydrogen phthalate (Kim et al. 2016), acetic acid (Šušnovská et al. 2012), Bis-Tris (based on our observation)) can interfere with absorbance measurements at this wavelength thus limiting the applicability of the method for pH

Table 1 Reported methods to measure LOX activity

Method	Working pH range	Linear detection range	Interference	Other limitations
Direct methods:				
Conjugated diene	Depends on the buffer selection	0–40 μ M (Pinto et al. 2007)	Chemicals used for buffer preparation, e.g., citric acid, acetic acid, Bis-Tris	Different response of different FAHPs (Browne and Armstrong 1998)
O ₂ consumption	Independent of pH	n.r	n.r	Low throughput
Indirect methods:				
Bleaching assay	n.r	n.r	Pigments (Romero and Barrett 1997)	–
Fluorescein	pH > 6.4 (Le Guern et al. 2020)	n.r	Antioxidants, reducing agents, and radical scavengers (Whent et al. 2010)	–
MBTH-DMAB	n.r	0–35 μ M (Anthon and Barrett 2001)	n.r	Sensitive to the changes in the Hb-LOX ratio (Anthon and Barrett 2001), Hb has a quasi-LOX activity (Kuhn et al. 1981)
FOX assay	n.r	0–25 μ M (Pinto et al. 2007)	n.r	Low linear detection ranges (Nielsen et al. 2003; Pinto et al. 2007), different response of different hydroperoxides (Jiang et al. 1992; Gay et al. 1999a; Vega et al. 2005)

n.r. not reported

optimum screening. Moreover, different FAHPs have varying extinction coefficients (Browne and Armstrong 1998), which makes direct comparison of LOX activity toward different PUFAs challenging, unless all respective standards are available. Another common direct method for determining LOX activity is by measuring oxygen consumption using an oxygen electrode. This method allows for LOX activity to be measured independently of the buffer used (Berkeley and Galliard 1976). However, the disadvantage of this method is its low throughput, limiting its application for rapid screening of many samples.

In addition to these direct methods, some indirect methods have been developed for the rapid measurement of LOX activity. Bleaching assays are used to assess the ability of LOX enzymes to bleach dyes (Romero and Barrett 1997; Qian et al. 2017; Lu et al. 2020). In these assays, LOX oxidizes fatty acids to FAHPs, which subsequently oxidize the dye. However, the sensitivity of bleaching assays is affected by the presence of impurities in the enzyme solution, i.e., pigments (Romero and Barrett 1997), therefore limiting its application for screening the activity of crude LOXs sourced from plants. Another indirect method using fluorescein has shown excellent reproducibility, accuracy, and precision (Whent et al. 2010). Fluorescein has been proposed to act as a scavenger by reacting with the peroxy radical (ROO•)

formed during reactions catalyzed by LOX, which can be monitored by looking at the decrease in fluorescein fluorescence (Whent et al. 2010). Nevertheless, fluorescein can only be used in a pH range above its pK_a value of 6.4. At lower pH values, the protonated forms of fluorescein become non-fluorescent (Le Guern et al. 2020), thus limiting the use of this method for pH optimum screening. In another indirect method, FAHPs produced by LOX act as oxidants, while hemoglobin (Hb) acts as a catalyst for oxidative coupling of 3-methyl-2-benzothiazolinone hydrazone (MBTH) with 3-(dimethylamino)benzoic acid (Anthon and Barrett 2001). The resulting reaction produces a purple color that can be detected spectrophotometrically. Even though the method was shown to give comparable results to the conjugated diene method, the sensitivity to changes in the Hb-LOX ratio makes this method hard to apply, especially when an unknown concentration of LOX or impure LOX is used (Anthon and Barrett 2001). Moreover, Hb has been reported to have quasi-LOX activity when a high concentration of substrate is used (i.e., more than 0.1 mM linoleic acid) and the reaction is measured at a pH between 7 and 9 (Kuhn et al. 1981), increasing the complexity of the method and making it unsuitable for optimum pH screening of LOXs.

Among the indirect methods, the ferrous oxidation–xylenol orange (FOX) assay has been reported as a sensitive

method applicable for high-throughput screening of LOX activity (Waslidge and Hayes 1995; Cho et al. 2006; Li and Schwarz 2018), which can detect up to 1.0–2.5 μM of FAHPs (Cho et al. 2006; Pinto et al. 2007). The assay is a widely used method to determine the hydroperoxide content of biological and food samples (Bou et al. 2008), as well as to assess the activity of LOX extracted from plant and animal material (Vega et al. 2005; Pinto et al. 2007; Fukuzawa et al. 2009; Timabud et al. 2013). The assay is based on the oxidation of ferrous iron (Fe^{2+}) to ferric iron (Fe^{3+}) by FAHPs produced by LOX. The resulting ferric iron subsequently forms a complex with xylenol orange (Fe^{3+} -XO complex) which gives a visible purple color and absorbs strongly at 550–580 nm (Bou et al. 2008). To obtain accurate results, it is crucial to conduct the FOX assay under acidic conditions. This is necessary because ferrous ions tend to rapidly convert to ferric ions in non-acidic environments (Straub et al. 2001). By maintaining the reaction mixture under acidic conditions, the oxidation of ferrous ions occurs specifically due to the presence of hydroperoxides (Wolff 1994). This ensures that only the desired reaction takes place, leading to reliable and accurate results in the assay. The effect of different acids on the sensitivity of the assay has been evaluated (Gay et al. 1999a; Gay and Gebicki 2002; Vega et al. 2005). Perchloric acid was proposed to be more suitable than sulfuric acid because it decreases the sensitivity to pH shifts and increases the ability to tolerate the presence of biological materials (Gay and Gebicki 2002). When buffers with varying pH values are used for pH optimum screening of LOX activity, the final pH of the reaction mixture might be slightly altered and thereby the sensitivity of the assay may be affected. However, the applicability of this method across a wide range of sample pH has not been evaluated yet.

A current limitation of the FOX assay is its low linear detection range (Nielsen et al. 2003; Pinto et al. 2007), which is unfavorable for accurately measuring LOX-produced FAHPs, especially when their concentration is expected to be high. At such elevated levels, accurate measurements become impossible since they exceed the detection limit of the assay. In addition, attempting to stop the enzymatic reaction and dilute the sample afterward is not a feasible solution due to the instability of FAHPs (Griffiths et al. 2000; Musakhanian et al. 2022). As a result of this restricted linear detection range, adjustments to the enzymatic reaction mixture become necessary, such as modifying the enzyme and/or substrate concentrations and/or incubation time, to facilitate the quantification of the generated FAHPs. Adjustments of those abovementioned conditions take effort and time, especially when the activity of the LOX of interest is unknown, which affects the simplicity of the assay. Therefore, it is important to find a way to extend the linear detection range. Another potential limitation of the FOX assay

is that different hydroperoxide species can exhibit different reactivity toward the xylenol orange reagent (Jiang et al. 1992; Gay et al. 1999a; Vega et al. 2005), causing difficulties for the accurate quantification of multiple different LOX-produced FAHPs. So far, cumene hydroperoxide (CuHP) is the most commonly used standard compound for calibration in the FOX assay. However, it shows a different response compared to the tested FAHPs, i.e., the response of linoleic acid hydroperoxide is 54% higher than that of CuHP, while those of linolenic and arachidonic acid hydroperoxide are 18% and 27% lower than that of CuHP, respectively (Vega et al. 2005). Evaluation of the response of other FAHP species has not been reported yet.

In this study, we report a modification of the FOX assay. By increasing the concentration of perchloric acid used in the FOX reagent, we aim at extending the linear detection range of hydroperoxides. This is because at very acidic conditions, ferrous iron becomes less prone to oxidation and xylenol orange becomes fully protonated (Liosi et al. 2017). This slows down the complexation reaction and reduces the sensitivity of the assay. In order to maintain a comparable level of detection, higher concentrations of hydroperoxides are required, thereby extending the linear detection range. Optimization of the perchloric acid concentration is necessary to strike a balance between expanding the linear detection range of hydroperoxides while maintaining sufficient sensitivity. In this study, we tested four different perchloric acid concentrations to evaluate the sensitivity and linear detection range of the assay. We also assessed the capability of the modified FOX assay to measure hydroperoxides in samples with a wide range of pH values. Furthermore, we evaluated the assay's ability to measure different hydroperoxide species, which is of importance for its applicability for screening the substrate specificity of LOXs. Finally, we compared the performance of the modified FOX assay in determining FAHP produced by a bacterial LOX to the commonly used conjugated diene method.

Materials and methods

Materials

Chemicals used for enzymatic reactions and FOX assay were obtained from the following sources: linoleic acid (LA; C18:2 $\Delta 9Z,12Z$) from Nu-Chek Prep, Inc., Minnesota, USA; fatty acid hydroperoxide standards (13(*S*)-hydroperoxy-9Z,11*E*-octadecadienoic acid (13-HPODE), 13(*S*)-hydroperoxy-9Z,11*E*,15*Z*-octadecatrienoic acid (13-HPOTE), 15(*S*)-hydroperoxy-5Z,8Z,11Z,13*E*-eicosatetraenoic acid (15-HPETE), 12(*S*)-hydroperoxy-5Z,8Z,10*E*,14Z,17*Z*-eicosapentaenoic acid (12-HPEPE), and 17(*S*)-hydroperoxy-4Z,7Z,10Z,13Z,15*E*,19*Z*-docosahexaenoic acid

(17-HPDHE)) from Larodan, Solna, Sweden; xylenol orange tetrasodium salt, iron(II) sulfate heptahydrate, cumene hydroperoxide (CuHP), hydrogen peroxide (HP), and perchloric acid from Sigma-Aldrich, Missouri, USA.

The gene of *Burkholderia thailandensis* lipoxigenase (Bt-LOX) (An et al. 2015) (NCBI ABC36974.1) with codons optimized for expression in *Escherichia coli* (Table S1) was purchased from GenScript Biotech, The Netherlands. The gene was obtained in a pET-19b plasmid (Novagen, USA), inserted between the *NdeI* and *BlnI* restriction sites. A 10×His-tag was present at the N terminus of the enzyme and was used for protein purification. Materials used for the enzyme production and purification were obtained from the following sources: *Escherichia coli* BL21(DE3) competent cells from Invitrogen, California, USA; Luria Bertani medium, pepstatin A, and ampicillin sodium salt from Sigma-Aldrich, Missouri, USA; isopropyl β-D-1-thiogalactopyranoside (IPTG) from Duchefa Biochemie B.V., Haarlem, The Netherlands; BugBuster master mix and Ni-NTA His-bind resin from Millipore-Merck, Darmstadt, Germany; cOmplete mini EDTA-free protease inhibitor cocktail from Roche, Mannheim, Germany; VivaSpin spin filters from GE Healthcare, Buckinghamshire, UK.

Protein expression and purification

Recombinant *E. coli* BL21(DE3) transformed with the pET-19b_Bt-LOX plasmid was cultivated in Luria Bertani medium at 37 °C with shaking at 250 rpm. When the optical density of the bacterial culture at 600 nm (OD_{600}) reached 0.6–0.8, 0.5 mM IPTG was added and the culture was further incubated at 16 °C with shaking at 150 rpm for 48 h. Then, the cells were harvested by centrifugation at $7000 \times g$ for 15 min at 4 °C and stored at –20 °C until protein purification.

To purify the Bt-LOX enzyme, a lysis solution was first added to the frozen cell pellet obtained from 200 mL culture medium. The lysis solution consisted of one Mini EDTA-free cOmplete protease inhibitor cocktail tablet and 1 μM pepstatin A dissolved in 10 mL of BugBuster Master Mix. Centrifugation at $16,000 \times g$ for 20 min at 4 °C was carried out to remove cell debris, and the resulting supernatant was filtered using a 0.22-μm membrane filter. Subsequently, purification was conducted using a gravity flow column containing 1 mL of Ni-NTA His-bind resin. Prior to sample application, the column was equilibrated with 10 column volumes (CV) of an equilibration buffer consisting of 50 mM NaH_2PO_4 , 300 mM NaCl, and 10 mM imidazole adjusted to pH 7.0 with a 1 M HCl solution. The filtered supernatant was then applied to the column, which was subsequently washed with 2 CV each of four washing buffers pH 7, containing 50 mM NaH_2PO_4 , 300 mM NaCl,

and increasing concentrations of imidazole of 20, 50, 100, and 150 mM, respectively. Elution of the purified enzyme was achieved using 4 CV of elution buffer pH 7, containing 50 mM NaH_2PO_4 , 300 mM NaCl, and 250 mM imidazole. The desalting of the elution fractions was performed using a VivaSpin spin filter with a molecular weight cut-off of 10 kDa. The purified enzyme was stored in 100 mM phosphate buffer pH 7, its concentration was determined using the BCA assay, and its size was confirmed by SDS-PAGE, showing a single band at approximately 75 kDa.

Absorption spectral analysis of the ferric-xylenol orange complex

The FOX assay was carried out with some modifications of the previously described method (Gay and Gebicki 2002; Pinto et al. 2007). The xylenol orange reagent containing 2.0 mM ferrous sulfate, 0.29 mM xylenol orange tetrasodium salt, and 440 mM perchloric acid in methanol/water (9:1) was freshly prepared. To find the optimum absorbance at which the concentration of the ferric-xylenol orange (Fe^{3+} -XO) complex can be determined, 30 μL of cumene hydroperoxide (0–10.52 mM dissolved in water) and 150 μL xylenol orange reagent were mixed well. The mixtures were then incubated for 15 min at room temperature (~20 °C) and the absorption spectra of the mixtures were measured in the wavelength range of 400–650 nm using a Spectramax ID3 multi-detection microplate reader (Molecular Devices, LLC, San Jose, California, USA). When the absorbance of the samples exceeded 2.0, the samples were diluted in 75% methanol in water. The actual absorbance of the sample was then calculated, taking the dilution factor into account.

Optimization of perchloric acid concentration and its effect on the linear detection range of hydroperoxides

To study the effect of perchloric acid concentration on the linear detection range of the FOX assay, xylenol orange reagent was freshly prepared using different concentrations of perchloric acid. The xylenol orange reagent contained 2.0 mM ferrous sulfate, 0.29 mM xylenol orange tetrasodium salt, and perchloric acid (110, 220, 440, or 660 mM) diluted in methanol/water (9:1). The assay was carried out by mixing 30 μL of the sample and 150 μL xylenol orange reagent in a 96-well microplate. The mixture was then incubated for 15 min at room temperature. The absorbance of the samples was read at 570 nm using the Spectramax ID3 multi detection microplate reader. The concentration of perchloric acid which offers a broader linear detection range while maintaining sufficient sensitivity for the measurement (440 mM) was then selected for further experiments.

Evaluation of the modified FOX assay on different sample pHs and different hydroperoxide species

The effect of the sample pH on the modified FOX assay was evaluated by performing the assay on CuHP calibration curves (0–175.2 μM) diluted in different buffers. The buffers used were 100 mM citrate pH 3.0, 4.0, and 5.0, 100 mM Bis–Tris pH 6.0 and 7.0, and 100 mM Tris–HCl pH 8.0, 9.0, and 10.0. The effect of different hydroperoxide species on the response of the modified FOX assay was assessed by measuring various concentrations of the hydroperoxide species, i.e., CuHP, HP, 13-HPODE, 13-HPOTE, 15-HPETE, 12-HPEPE, and 17-HPDHE. For the sake of stability, all the hydroperoxide standard compounds were dissolved in methanol. When measuring different hydroperoxide species, the methanol/water ratio in the xylenol orange reagent was adjusted to 7:1. This adjustment ensured that the final methanol concentration in the reaction mixture remained consistent with the standard protocol. The molar absorption coefficient (ϵ) of the Fe^{3+} –XO complex for each hydroperoxide was calculated using Eq. (1). The absorbance of the Fe^{3+} –XO complex at 570 nm (A) per concentration of the hydroperoxide (c) was determined from the slope of the linear part ($R^2 > 0.99$) of the calibration curve. The length of the light path through the solution (l) was determined by calculating the height of the sample solution in the 96-well microplate.

$$\epsilon = \frac{A}{lc} \quad (1)$$

Determination of Fe^{3+} /hydroperoxide ratio

The number of ferric ions generated by each –OOH group from different hydroperoxide species was expressed as the Fe^{3+} /hydroperoxide ratio. The calculation involved dividing the molar absorption coefficient of the Fe^{3+} –XO complex generated by the –OOH group in each hydroperoxide species by the molar absorption coefficient of the complex generated by ferric ions in the same reagent (Gay et al. 1999b, 1999a). The molar absorption coefficient of the Fe^{3+} –XO complex generated by ferric ions was determined by making a calibration curve of FeCl_3 from 0 to 120 μM .

Preparation of solubilized fatty acids

Solubilized LA was freshly prepared according to a previously described protocol with slight modifications (Axelrod et al. 1981). In a 10-mL volumetric flask, 13.5 μL LA was mixed with 12.5 μL of Tween-20 in 4 mL milli-Q water. After adding 0.55 mL of 0.5 M NaOH, the solution became clear, and milli-Q water was added to adjust the volume to 10 mL, resulting in a final LA concentration of 4.3 mM.

Comparison between FOX assay and conjugated diene method

To validate the accuracy of the modified FOX assay, fatty acid hydroperoxide produced from LA by Bt-LOX was measured using two different methods, i.e., FOX assay and conjugated diene method. Solutions containing 13.25 nM Bt-LOX, LA in the range of 4.3–139 μM , and 100 mM buffer pH 6 were used as the enzymatic reaction mixtures. Bis–Tris buffer was used for the FOX assay, while phosphate buffer was used for the conjugated diene method to prevent any interference from absorption by the buffer. The reaction mixtures were homogenized and incubated for 5 min at 25 °C. LOX activity measured based on the FOX assay was performed as described above; 13-HPODE (LA-derived hydroperoxide) was used as the standard for the calibration curve. Concentration of fatty acid hydroperoxide based on the conjugated diene method was determined by measuring the absorbance at 234 nm during 5-min incubation of the enzyme with LA using Jasco V-730 UV–vis/NIR spectrophotometer (Jasco, Easton, Maryland, USA). The concentration of fatty acid hydroperoxide formed was calculated using a molar absorption coefficient of 25,000 $\text{M}^{-1} \text{cm}^{-1}$ (Axelrod et al. 1981).

Results

Absorption spectral analysis of the Fe^{3+} –XO complex

In the FOX assay, ferrous iron is oxidized to ferric iron in the presence of hydroperoxides, which can then react with xylenol orange to form the Fe^{3+} –XO complex. To determine at which wavelength the Fe^{3+} –XO complex shows the highest absorbance and should therefore be measured in the assay, 0 to 10.52 mM of CuHP was incubated in the presence of xylenol orange reagent and the absorbance of the mixture was measured in the wavelength range of 400–650 nm. In the absence of CuHP, the absorption spectrum of XO exhibited two distinct peaks at 440 and 520 nm (Fig. 2), which agrees with previous reports (Timabud et al. 2013; Belleza and Villaraza 2014). The peak observed at 440 nm (dashed orange line), which indicates the presence of xylenol orange, has been frequently reported (Jiang et al. 1992; Hermes-Lima et al. 1995; Gay et al. 1999a; Timabud et al. 2013). On the other hand, the peak at 520 nm may indicate the formation of a complex between Fe^{2+} and XO (Fig. S1), as xylenol orange has also been reported to form complexes with divalent metal ions (Belleza and Villaraza 2014). The gradual increase in CuHP concentration led to a progressive shift in the maximum absorbance, starting from 520 nm and progressing to 530 nm, then to 560 nm, and

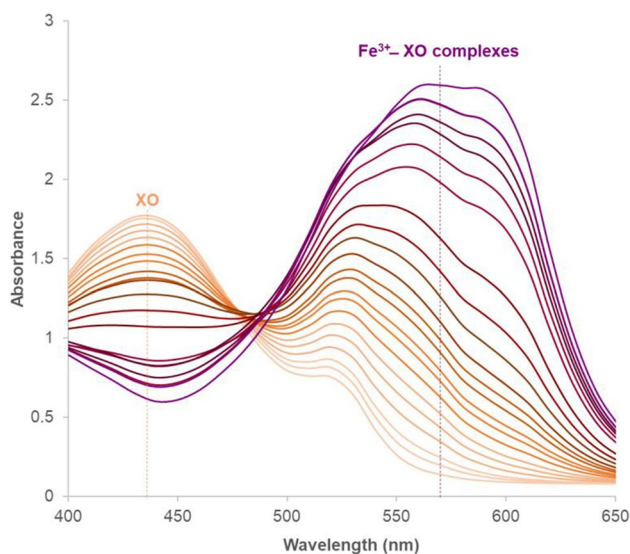


Fig. 2 Absorption spectra of xylenol orange reagent in the presence of cumene hydroperoxide at 0, 8.8, 17.5, 35.0, 52.6, 70.1, 87.6, 105.1, 122.7, 140.2, 157.7, 227.8, 262.8, 297.9, 368.0, 438.0, 525.7, 613.3, 788.5, 1226.5, and 10520.0 μM (shown as lines colored progressively from light orange to dark purple). Xylenol orange shows the highest peak centered at 440 nm (shown as lightest orange line) that decreases in the presence of cumene hydroperoxide due to the formation of Fe^{3+} –XO complexes, characterized by a progressive shift in the maximum absorbance, starting from 520 to 530 nm, then to 560 nm, and finally to 590 nm. Samples with absorbance values surpassing 2.0 were diluted in a 75% methanol–water solution, and the final absorbance was determined considering the dilution factor

finally to 590 nm (Fig. 2). The spectral shift toward higher wavelengths occurred due to the presence of CuHP, which oxidized ferrous iron to its ferric state leading to the formation of Fe^{3+} –XO complexes. The shift in the maximum absorbance to four distinct wavelengths suggests the existence of different Fe^{3+} –XO complexes at potentially four

different stoichiometric ratios: $(\text{Fe}^{3+})-(\text{XO})_3$, $(\text{Fe}^{3+})-(\text{XO})_2$, $(\text{Fe}^{3+})-(\text{XO})$, and $(\text{Fe}^{3+})_2-(\text{XO})$ (Yoshino et al. 1979; Liosi et al. 2017; Scotti et al. 2022). The formation of different Fe^{3+} –XO complexes is also indicated by the absence of an isosbestic point. Due to interference caused by the initial state of the xylenol orange reagent at 520 nm, the wavelength of 570 nm (indicated by the dashed purple line), which is near the midpoint between 560 and 590 nm, was chosen for further analysis. From this point onwards, the term “ Fe^{3+} –XO complex” will be used to indicate complexes formed at any stoichiometric ratio of Fe^{3+} and XO, without specifying which of the possible complexes are formed.

Effect of perchloric acid concentration on the linear detection range of hydroperoxides

The effect of perchloric acid concentration in the FOX reagent on expanding the linear detection range of hydroperoxides was evaluated. As hydroperoxide production by LOXs is commonly conducted in a buffered system, calibration curves of CuHP dissolved in various buffers were measured using xylenol orange reagent dissolved in different concentrations of perchloric acid (110, 220, 440, and 660 mM). The results showed that increasing the concentration of perchloric acid expands the linear detection range of CuHP in all the buffers and pH values tested. Figure 3a, b, and c illustrate the results for 100 mM citrate buffer pH 3.0, 100 mM Bis–Tris pH 6.0, and 100 mM Tris–HCl pH 9.0, respectively (the complete data set at all different pH values is shown in Fig. S2). Concentrations of 110 and 220 mM perchloric acid gave a comparable linear range for CuHP from 0 to 20–35 μM , depending on the pH and the type of buffer employed. This finding is similar to the previous report that xylenol orange with 110 mM perchloric acid gives a linear

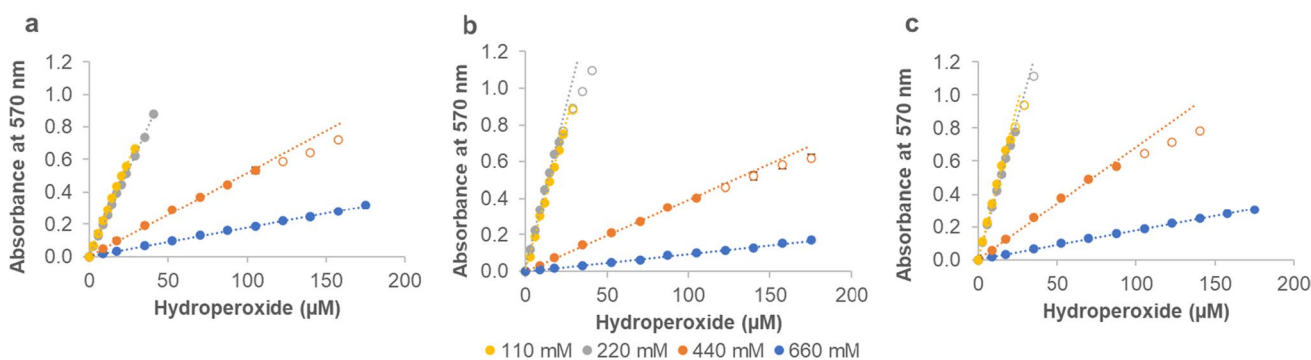


Fig. 3 Effect of perchloric acid concentration (110, 220, 440, and 660 mM) in the xylenol orange reagent on the linear detection range of cumene hydroperoxide diluted in different buffers. **a** 100 mM citrate buffer pH 3.0, **b** 100 mM Bis–Tris pH 6.0, and **c** 100 mM Tris–

HCl pH 9.0. The linear ranges (R^2 value > 0.99) are represented by filled circles, while datapoints outside the linear ranges are indicated by open circles of the same color. Data represent mean \pm SD ($n=3$). When not visible, the error bars are hidden below the markers

range for hydroperoxy linoleic acid from 0 to 25 μM (Pinto et al. 2007). Higher concentrations of perchloric acid of 440 and 660 mM gave broader linear ranges for CuHP from 0 to 88–105 μM and from 0 to 175 μM , respectively. However, the sensitivity of the method is diminished by the increased perchloric acid concentrations, as the molar absorption coefficient of the Fe^{3+} –XO complex decreases (Table 2). Depending on the pH and the type of buffer employed, the molar absorption coefficient of the Fe^{3+} –XO complex decreases up to five–ninefold at 440 mM perchloric acid and up to 15–34-fold at 660 mM perchloric acid compared to that in 110 mM perchloric acid. The gradual decrease in the sensitivity of detection with increasing concentration of perchloric acid has been previously reported for concentrations between 110 and 180 mM (Gay and Gebicki 2002). Altogether, 440 mM perchloric acid provided a wider linear range compared to lower concentrations, while maintaining sufficient sensitivity for the measurement (i.e., with a higher molar absorption coefficient compared to 660 mM perchloric acid). The very low measured absorbance at 570 nm under 660 mM perchloric acids concentration (less than 0.1 for some data points as presented in Fig. S3d) makes the measurement less reliable. For this reason, 440 mM perchloric acid concentration was used in the following experiments.

Effect of buffer type and pH on the molar absorption coefficient of the Fe^{3+} –XO complex

To test the applicability of the modified FOX assay to screen for the pH optimum of LOXs, the method was applied to CuHP standard samples prepared in different buffers covering a wide pH range (Fig. S3). A linear range was observed for CuHP at all tested sample pH values (pH 3–10), suggesting that the FOX assay is suitable for measuring the formation of hydroperoxides over a broad range of sample pH (Fig. 4). However, the sensitivity of the assay depends on the type of sample buffer used and its pH. Different types of buffer yielded different molar absorption coefficients for the Fe^{3+} –XO complex. In addition, lowering the sample

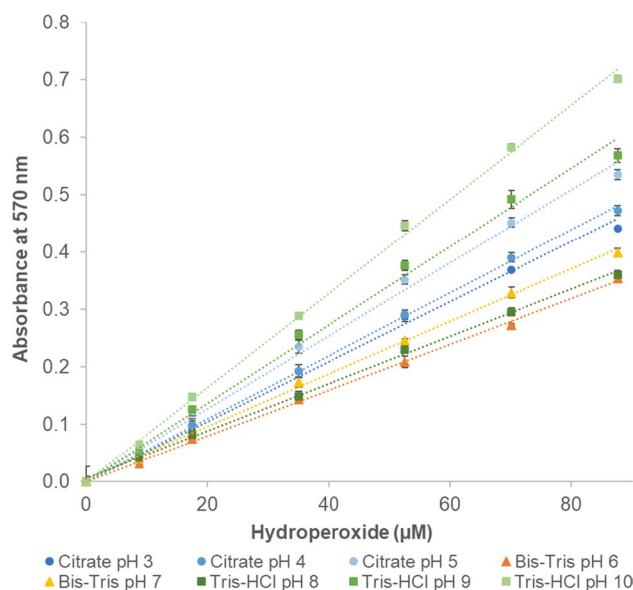


Fig. 4 Standard curves of cumene hydroperoxide diluted in different buffers measured by FOX assay. All the buffers used had a concentration of 100 mM. FOX reagent was prepared using 440 mM perchloric acid. Data represent mean \pm SD ($n=3$). When not visible, the error bars are hidden below the markers

pH within the same buffer type resulted in a decrease in the molar absorption coefficient of the Fe^{3+} –XO complex (Table 2).

Sensitivity of the modified FOX assay toward different hydroperoxides species

To investigate the sensitivity of the modified FOX assay toward different hydroperoxide species, we measured various concentrations of FAHPs, CuHP, and HP using this assay. The results showed that different hydroperoxide species exhibit different reactivity in the modified FOX assay (Fig. 5), which is indicated by different molar absorption coefficients between the hydroperoxide species (Table 3).

Table 2 Molar absorption coefficients of the Fe^{3+} –XO complex for cumene hydroperoxide in presence of various buffer types at different pH values measured by FOX assay using various concentrations of perchloric acid

Buffer	Molar absorption coefficient of Fe^{3+} –XO complex at 570 nm ($\text{M}^{-1} \text{cm}^{-1}$)			
	110 mM*	220 mM*	440 mM*	660 mM*
Citrate pH 3	51,068 \pm 514	46,460 \pm 620	10,597 \pm 243	3,726 \pm 68
Citrate pH 4	63,774 \pm 1091	61,131 \pm 509	11,456 \pm 169	3,828 \pm 66
Citrate pH 5	62,708 \pm 1076	61,553 \pm 1206	13,033 \pm 225	4,029 \pm 44
Bis–Tris pH 6	68,258 \pm 3101	64,479 \pm 503	8,185 \pm 102	2,011 \pm 67
Bis–Tris pH 7	88,067 \pm 922	70,427 \pm 658	9,533 \pm 63	3,047 \pm 53
Tris–HCl pH 8	61,173 \pm 563	56,527 \pm 382	8,529 \pm 115	2,539 \pm 12
Tris–HCl pH 9	77,584 \pm 1654	70,907 \pm 1160	14,074 \pm 65	3,688 \pm 20
Tris–HCl pH 10	92,930 \pm 1455	73,804 \pm 678	17,147 \pm 219	4,915 \pm 91

*Concentration of perchloric acid used in the xylenol orange reagent. Data represent mean \pm SD ($n=3$)

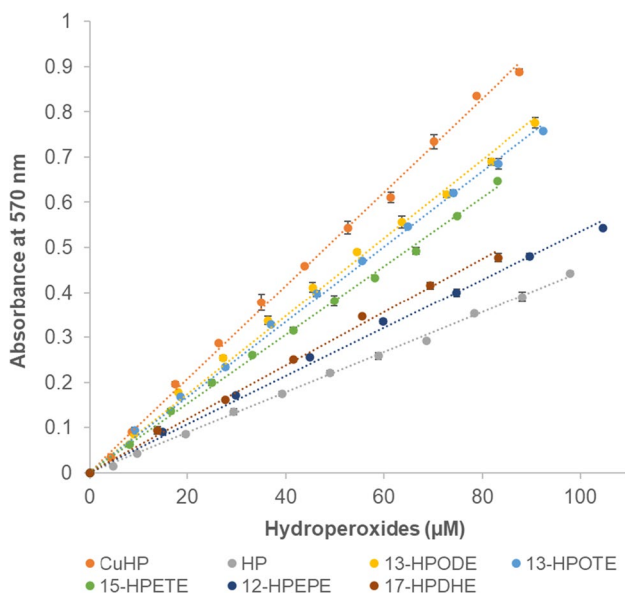


Fig. 5 Standard curves of different hydroperoxides measured by the FOX assay using 440 mM of perchloric acid. CuHP: cumene hydroperoxide, HP: hydrogen peroxide, 13-HPODE: 13(*S*)-hydroperoxy-9*Z*,11*E*-octadecadienoic acid, 13-HPOTE: 13(*S*)-hydroperoxy-9*Z*,11*E*,15*Z*-octadecatrienoic acid, 15-HPETE: 15(*S*)-hydroperoxy-5*Z*,8*Z*,11*Z*,13*E*-eicosatetraenoic acid, 12-HPEPE: 12(*S*)-hydroperoxy-5*Z*,8*Z*,10*E*,14*Z*,17*Z*-eicosapentaenoic acid, and 17-HPDHE: 17(*S*)-hydroperoxy-4*Z*,7*Z*,10*Z*,13*Z*,15*E*,19*Z*-docosahexaenoic acid. Error bars represent mean \pm SD ($n=3$). When not visible, the error bars are hidden below the markers

To understand this phenomenon, the amount of ferric ions formed per hydroperoxide molecule was estimated for each species. To achieve this, the molar absorption coefficients of Fe^{3+} -XO complexes generated by each hydroperoxide species were compared to the molar absorption coefficients

of Fe^{3+} -XO complexes that were generated using known quantities of $FeCl_3$ (Table 3).

Comparison of the FOX assay with conjugated diene method

To validate the accuracy of the modified FOX assay and its applicability to measure the activity of LOX enzymes, hydroperoxides produced through the enzymatic conversion of linoleic acid by Bt-LOX were measured with the modified FOX assay and the results were compared with those obtained using the well-established method based on measuring the absorbance of the conjugated diene moiety of the formed FAHPs. The enzymatic reaction conditions were set to obtain full or almost full conversion of the substrate, as observed from a plateau of the curve in the conjugated diene measurement at 234 nm (Fig. S4). The end-point measurement of hydroperoxide concentrations using the two different methods was compared (Table S2) and the results are shown in Fig. 6. A high correlation between hydroperoxide concentrations measured by the modified FOX assay and the conjugated diene method was observed, confirming that the modified FOX assay method is an accurate method to measure LOX activity.

Discussion

In this study, we modified the FOX assay and evaluated its capacity to be used for rapid screening of LOX activity. The limited linear detection range of the FOX assay, as indicated by previous research (Nielsen et al. 2003; Pinto et al. 2007), poses a disadvantage when it comes to the quantification of LOX-produced FAHPs. In order to broaden the linear

Table 3 Molar absorption coefficients of the ferric ion-xylene orange complex generated by different hydroperoxides and the amount of Fe^{3+} ions generated per mole of hydroperoxide

Hydroperoxide species	Molar absorption coefficient Fe^{3+} -XO complex ($M^{-1} cm^{-1}$)	Fe^{3+} /hydroperoxide ratio*			
		This study	(Vega et al. 2005)	(Gay and Gebicki 2002)	(Gay et al. 1999a)
CuHP	21,823 \pm 238	5.8	5.6	5.8	5.4
HP	9,632 \pm 240	2.5		2.9	2.4
13-HPODE	17,711 \pm 165	4.7	8.6		2.0
13-HPOTE	17,068 \pm 90	4.5	4.6		
15-HPETE	15,838 \pm 93	4.2	4.1		
12-HPEPE	11,060 \pm 186	2.9			
17-HPDHE	12,307 \pm 138	3.3			

*The ratio of Fe^{3+} /hydroperoxide is defined as the number of Fe^{3+} ions generated by each hydroperoxide species. It was calculated from six experiments by dividing the molar absorption coefficient of the Fe^{3+} -XO complex generated by each hydroperoxide species by the molar absorption coefficient of the complex generated by ferric ions (from $FeCl_3$) in the same reagent (Gay et al. 1999b, 1999a). Please note that the Fe^{3+} /hydroperoxide ratio values obtained from the references were determined using different compositions of the FOX reagent. The molar absorption coefficient of each hydroperoxide represents mean \pm SD ($n=6$)

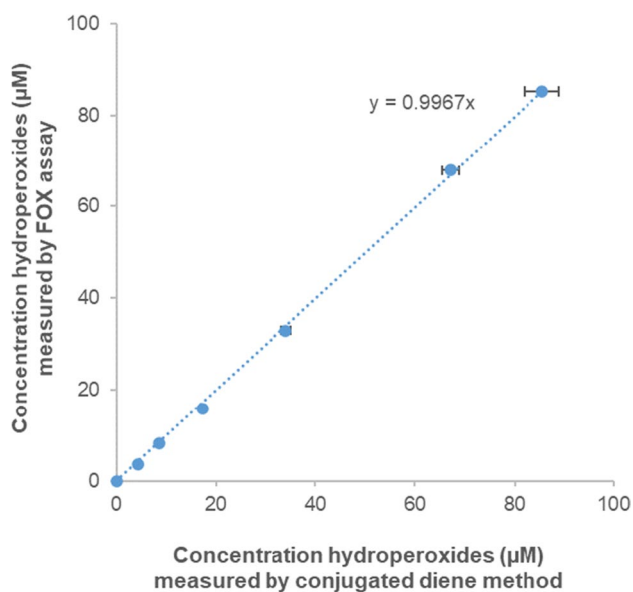


Fig. 6 Correlation between the measurement of hydroperoxides produced by conversion of linoleic acid by *B. thailandensis* LOX using the FOX assay and the conjugated diene method. Error bars represent mean \pm SD ($n=3$). When not visible, the error bars are hidden below the markers. Exact concentrations and standard deviations can be found in Table S2

detection range of hydroperoxides, the perchloric acid concentration in the FOX reagent was increased compared to the previously reported optimal concentration of 110 mM (Gay and Gebicki 2002). When higher concentrations of perchloric acid are used, ferrous iron becomes less susceptible to oxidation and xylenol orange becomes fully protonated which will slow down the complexation reaction. To reach a similar level of absorbance, higher concentrations of hydroperoxides are needed, which consequently leads to the expansion of the linear detection range. To strike a balance between expanding the linear detection range of hydroperoxides and ensuring adequate assay sensitivity, optimization of the perchloric acid concentration in the FOX reagent was performed. The modification of the FOX assay, by increasing the perchloric acid concentration to 440 mM, has successfully expanded the linear range of hydroperoxide quantification up to fivefold compared to the previously established FOX assay. Importantly, this modification has maintained the molar absorption coefficient of the Fe^{3+} -XO complex at a reasonable level, ensuring reliable and precise quantification of hydroperoxides. For instance, the modified FOX assay has demonstrated the ability to quantify down to 4.4 μM of linoleic acid hydroperoxide, as indicated in Table S2. If extremely sensitive detection is required, it is advisable to use 110 mM perchloric acid in the xylenol orange reagent.

To evaluate the applicability of the modified FOX assay for the pH optimum screening of LOXs, the method was

applied to CuHP standard samples prepared in different buffers covering a wide pH range. Selection of the buffer used for the enzymatic reaction monitored using the FOX assay is important. Besides not inhibiting the enzyme, the buffer should not contain any compounds that inhibit ferrous oxidation and Fe^{3+} -XO complexation. Compounds containing phosphate groups, for example, should be avoided, as they can bind either to the ferrous ion or the ferric ion to form iron salts, thus inhibiting ferrous oxidation and the formation of Fe^{3+} -XO complex (Tadolini and Sechi 1987; Wang et al. 2021). The modified FOX assay demonstrated applicability across a wide pH range, from pH 3 to 10. Nevertheless, the sensitivity of the assay depends on the type of sample buffer used and its pH. Lowering the sample pH within the same buffer type resulted in a decrease in the molar absorption coefficient of the Fe^{3+} -XO complex. In the case of Tris-HCl buffer from pH 10 to 8 and of Bis-Tris buffer from pH 7 to 6, for example, the reduction in molar absorption coefficient may be attributed to the use of hydrochloric acid for pH adjustment during buffer preparation. This is because chloride ions can coordinate with both ferrous and ferric ions in organic solvents (in this case in methanol/water 9:1) to form ferrous/ferric-chloride complexes (Inoue et al. 2022), thereby inhibiting the oxidation of ferrous iron and the formation of the Fe^{3+} -XO complex. Another possible explanation is that sample buffers with different pH values, when added to the assay reagent, may slightly affect the final pH of the assay mixture. It has indeed been reported that the color development in the FOX assay is influenced by the pH of the reaction mixture. For instance, when using 25 mM sulfuric acid in the xylenol orange reagent, the optimal pH for maximum color development was found to be 1.7–1.8 (Banerjee et al. 2003). When using perchloric acid at 110 mM in the xylenol orange reagent, the pH of the reaction mixture is 1.1 (Gay and Gebicki 2002). In this study, when using 440 mM perchloric acid in the xylenol orange reagent, the final pH of the reaction mixtures ranged from 0.50 to 0.60, depending on the buffer type and its pH (Fig. S5). This suggests that the pH of the reaction mixture may not fall within the optimal range for color development. In addition, evaluating the effect of the final pH of the mixture on color development is challenging, as different types of buffers yielded different responses (Fig. S5). Overall, the modified FOX assay has demonstrated its capability to measure hydroperoxides across a wide range of sample pH; it is, however, important to use a standard curve prepared in the same buffer as used in the sample due to the sensitivity of the assay to the type of sample buffer and its pH.

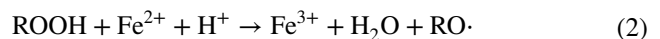
The reliability of measuring FAHPs produced by LOX using the previously established FOX assay is limited due to the varying reactivity of different FAHP species (such as linoleic, linolenic, and arachidonic hydroperoxides) compared to the commonly used standard compounds, like

CuHP and HP (Gay et al. 1999a; Vega et al. 2005). Notably, the response of other FAHP species has not been reported yet. To investigate the sensitivity of the modified FOX assay toward different hydroperoxide species, various concentrations of FAHPs, CuHP, and HP have been measured. The results showed that the modified FOX assay is capable of measuring various hydroperoxide species, thus, the method can be used effectively for screening substrate preference of LOXs. Nevertheless, different hydroperoxide species exhibit different reactivity in the modified FOX assay due to the different number of ferric ions generated by each –OOH group. The number of ferric ions generated by each –OOH group from different hydroperoxide species can be explained based on the reaction pathways of hydroperoxides in the presence of Fe^{2+} . Three categories of hydroperoxides can be distinguished (Gay et al. 1999a). The first class produces approximately 2.5 mol of ferric ions per mole of hydroperoxide, with hydrogen peroxide being the only member reported in this class (Gay et al. 1999a). Hydrogen peroxide oxidizes ferrous ions to ferric ions while generating hydroxy radicals. The hydroxy radical ($\text{HO}\bullet$) then reacts with xylenol orange to form xylenol orange-hydroxy radical ($\text{HOXO}\bullet$), which subsequently oxidizes ferrous ions to ferric ions (Gay et al. 1999a). In addition, the $\text{HO}\bullet$ can directly oxidize ferrous ions to ferric ions. However, the previous proposed mechanism (Gay et al. 1999a) does not adequately explain the generation of 2.5 mol of ferric ions per mole of hydrogen peroxide. We suggest that other reactions (e.g., via electron transfer from $\text{HO}\bullet$ to form $\text{XO}\bullet$, followed by O_2 coupling to the formed $\text{XO}\bullet$) contribute to the generation of > 2 of ferric ions per hydrogen peroxide molecule. However, the exact mechanism remains to be studied. The second class produces approximately 2.0 mol of ferric ions per mole of hydroperoxide, as previously reported for bovine serum albumin hydroperoxide (Gay et al. 1999a). In this class, each hydroperoxide molecule first oxidizes one ferrous ion to a ferric ion, generating an alkoxy radical ($\text{RO}\bullet$). The $\text{RO}\bullet$ then oxidizes another ferrous ion to a ferric ion, yielding an alcohol (ROH). The third class produces more than 2.5 mol of hydroperoxide, but the underlying mechanisms of these reactions have not been revealed yet. This class is represented, for example, by CuHP and *t*-butyl hydroperoxide (Gay et al. 1999a).

Based on our results, HP yielded 2.5 ferric ions (Table 3), which is in agreement with a previous report that found values between 2.2 and 2.7 depending on the acid used in the xylenol orange reagent (Gay et al. 1999a), and CuHP generated 5.8 ferric ions per mole of hydroperoxide (Table 3); this is in accordance with some previous reports that classified CuHP as belonging to the third class of hydroperoxides (Gay et al. 1999a; Gay and Gebicki 2002; Vega et al. 2005). Finally, the various FAHPs tested, which differed in carbon chain length and amount of double bonds, generated

different amounts of ferric ions. 13-HPODE, 13-HPOTE, and 15-HPETE generated 4.2–4.7 ferric ions per mole of hydroperoxide, while 12-HPEPE and 17-HPDHE produced respectively 2.9 and 3.3 ferric ions per mole of hydroperoxide. These results indicated that all tested FAHPs belong to the third class of hydroperoxides. Variation in the number of ferric ions generated by each –OOH group in FAHP was also observed across different studies for 13-HPODE. However, the reason for this variation remains unclear.

A possible mechanistic explanation for why all the tested FAHPs produced more than 2.5 ferric ions per mole of hydroperoxide is that the alkoxy radicals ($\text{RO}\bullet$) formed during the colorimetric assay (Gay et al. 1999a) (Eq. 2) rearrange to form carbon-centered alcohol radicals ($\bullet\text{ROH}$) (Eq. 3), which, in the presence of oxygen and under acidic conditions, can oxidize ferrous ion and yield a stoichiometric amount of hydrogen peroxide (Eq. 4) (Fig. 7). This hydrogen peroxide can then produce 2.5 additional ferrous ions as previously described. It is important to note that the reaction pathway shown in Fig. 7 is a simplification, and in practice, radicals might rearrange to form a more complex collection of products, as described in Fig. S6. The type of radical rearrangements that occur will affect the amounts of ferric ions generated. So, depending on the relative contribution of the individual reaction pathways from each of the FAHPs, theoretically 2.0–6.5 ferric ions can be formed. To fully rationalize the amount of ferric ions generated by the different hydroperoxides, the relative contribution of all different reaction pathways should be evaluated, which is beyond the scope of this study.



Overall, the modified FOX assay has demonstrated its ability to measure various hydroperoxide species. However, the sensitivity of the assay toward different hydroperoxide species necessitates calibration using the respective standard compound. When financial constraints hinder the use of FAHPs standard compounds during routine substrate preference screening for LOX activity, the use of a correction factor can be considered. To do so, determination of the molar absorption coefficient of the appropriate standard FAHP under the applied conditions should initially be performed together with another standard (e.g., CuHP or HP) using the same FOX reagent. Following this, CuHP or HP can be used as the standard for routine analysis for measuring LOX activity, with the FAHP concentration being calculated using a correction factor based on its molar absorption coefficient. An example of the application of correction factors in

References

- An JU, Kim BJ, Hong SH, Oh DK (2015) Characterization of an omega-6 linoleate lipoxygenase from *Burkholderia thailandensis* and its application in the production of 13-hydroxyoctadecadienoic acid. *Appl Microbiol Biotechnol* 99:5487–5497. <https://doi.org/10.1007/s00253-014-6353-8>
- An JU, Hong SH, Oh DK (2018) Regiospecificity of a novel bacterial lipoxygenase from *Myxococcus xanthus* for polyunsaturated fatty acids. *Biochim Biophys Acta Mol Cell Biol Lipids* 1863:823–833. <https://doi.org/10.1016/j.bbalip.2018.04.014>
- Anthon GE, Barrett DM (2001) Colorimetric method for the determination of lipoxygenase activity. *J Agric Food Chem* 49:32–37. <https://doi.org/10.1021/jf000871s>
- Axelrod B, Cheesbrough TM, Laakso S (1981) Lipoxygenase from soybeans: EC 1.13.11.12 linoleate: oxygen oxidoreductase. *Methods Enzymol* 71:441–451. [https://doi.org/10.1016/0076-6879\(81\)71055-3](https://doi.org/10.1016/0076-6879(81)71055-3)
- Banerjee D, Madhusoodanan UK, Sharanabasappa M, Ghosh S, Jacob J (2003) Measurement of plasma hydroperoxide concentration by FOX-1 assay in conjunction with triphenylphosphine. *Clin Chim Acta* 337:147–152. <https://doi.org/10.1016/J.CCCN.2003.08.004>
- Banthiya S, Kalmes J, Galemou Yoga E, Ivanov I, Carpena X, Hamberg M, Kuhn H, Scheerer P (2016) Structural and functional basis of phospholipid oxygenase activity of bacterial lipoxygenase from *Pseudomonas aeruginosa*. *Biochim Biophys Acta Mol Cell Biol Lipids* 1861:1681–1692. <https://doi.org/10.1016/j.bbalip.2016.08.002>
- Belleza OJV, Villaraza AJL (2014) Ion charge density governs selectivity in the formation of metal–xylenol orange (M–XO) complexes. *Inorg Chem Commun* 47:87–92. <https://doi.org/10.1016/J.INO-CHE.2014.07.024>
- Berkeley HD, Galliard T (1976) Measurement of lipoxygenase activity in crude and partially purified potato extracts. *Phytochemistry* 15:1475–1479. [https://doi.org/10.1016/S0031-9422\(00\)88919-0](https://doi.org/10.1016/S0031-9422(00)88919-0)
- Bou R, Codony R, Tres A, Decker EA, Guardiola F (2008) Determination of hydroperoxides in foods and biological samples by the ferrous oxidation-xylenol orange method: a review of the factors that influence the method's performance. *Anal Biochem* 377:1–15. <https://doi.org/10.1016/j.ab.2008.02.029>
- Browne RW, Armstrong D (1998) Separation of hydroxy and hydroperoxy polyunsaturated fatty acids by high-pressure liquid chromatography. *Methods Mol Biol* 108:147–155. <https://doi.org/10.1385/0-89603-472-0:147>
- Cho YS, Kim HS, Kim CH, Cheon HG (2006) Application of the ferrous oxidation-xylenol orange assay for the screening of 5-lipoxygenase inhibitors. *Anal Biochem* 351:62–68. <https://doi.org/10.1016/j.ab.2005.12.025>
- Chrisnasari R, Hennebelle M, Vincken J, Van BWJH, Ewing TA (2022) Bacterial lipoxygenases: biochemical characteristics, molecular structure and potential applications. *Biotechnol Adv* 61:108046. <https://doi.org/10.1016/j.biotechadv.2022.108046>
- Corongiu FP, Milia A (1983) An improved and simple method for determining diene conjugation in autoxidized polyunsaturated fatty acids. *Chem Biol Interact* 44:289–297. [https://doi.org/10.1016/0009-2797\(83\)90056-X](https://doi.org/10.1016/0009-2797(83)90056-X)
- Egmond MR, Vliegthart JFG, Boldingh J (1972) Stereospecificity of the hydrogen abstraction at carbon atom n-8 in the oxygenation of linoleic acid by lipoxygenases from corn germs and soya beans. *Biochem Biophys Res Commun* 48:1055–1060. [https://doi.org/10.1016/0006-291X\(72\)90815-7](https://doi.org/10.1016/0006-291X(72)90815-7)
- Fukuzawa K, Nano M, Akai K, Morishige J, Tokumura A, Jisaka M (2009) Measurement of lipid hydroperoxides by the ferric-xylenol orange method (2): application to lipoxygenase assay. *J Nutr Sci Vitaminol (tokyo)* 55:92–98. <https://doi.org/10.3177/jnsv.55.92>
- Gao Y, Zhang Y (2018) Formation and photochemical properties of aqueous brown carbon through glyoxal reactions with glycine. *RCS Adv* 8:38566–38573. <https://doi.org/10.1039/c8ra06913a>
- Gay CA, Gebicki JM (2002) Perchloric acid enhances sensitivity and reproducibility of the ferric–xylenol orange peroxide assay. *Anal Biochem* 304:42–46. <https://doi.org/10.1006/ABIO.2001.5566>
- Gay C, Collins J, Gebicki JM (1999a) Hydroperoxide assay with the ferric-xylenol orange complex. *Anal Biochem* 273:149–155. <https://doi.org/10.1006/ABIO.1999.4208>
- Gay C, Collins J, Gebicki JM (1999b) Determination of iron in solutions with the ferric-xylenol orange complex. *Anal Biochem* 273:143–148. <https://doi.org/10.1006/ABIO.1999.4207>
- Gigot C, Ongena M, Fauconnier ML, Wathelet JP, du Jardin P, Thonart P (2010) The lipoxygenase metabolic pathway in plants: potential for industrial production of natural green leaf volatiles. *Biotechnol Agron Soc Environ* 14:451–460
- Goloshchapova K, Stehling S, Heydeck D, Blum M, Kuhn H (2018) Functional characterization of a novel arachidonic acid 12S-lipoxygenase in the halotolerant bacterium *Myxococcus fulvus* exhibiting complex social living patterns. *Microbiol Open* 8:1–17. <https://doi.org/10.1002/mbo3.775>
- Griffiths G, Leverentz M, Silkowski H, Gill N, Sá Nchez-Serrano JJ (2000) Lipid hydroperoxide levels in plant tissues. *J Exp Bot* 51:1363–1370. <https://doi.org/10.1093/jexbot/51.349.1363>
- Hamberg M, Samuelsson B (1967) On the specificity of the oxygenation of unsaturated fatty acids catalyzed by soybean lipoxidase. *J Biol Chem* 242:5329–5335. [https://doi.org/10.1016/S0021-9258\(18\)99432-9](https://doi.org/10.1016/S0021-9258(18)99432-9)
- Hamberg M, Su C, Oliw E (1998) Manganese lipoxygenase. Discovery of a bis-allylic hydroperoxide as product and intermediate in a lipoxygenase reaction. *J Biol Chem* 273:13080–13088. <https://doi.org/10.1074/JBC.273.21.13080>
- Hermes-Lima M, Willmore WG, Storey KB (1995) Quantification of lipid peroxidation in tissue extracts based on Fe(III)xylenol orange complex formation. *Free Radic Biol Med* 19:271–280. [https://doi.org/10.1016/0891-5849\(95\)00020-X](https://doi.org/10.1016/0891-5849(95)00020-X)
- Hu J, Jin Z, Chen TY, Polley JD, Cunningham MF, Gross RA (2014) Anionic polymerizable surfactants from biobased ω-hydroxy fatty acids. *Macromolecules* 47:113–120. <https://doi.org/10.1021/MA401292C>
- Inoue D, Komatsu T, Niwa H, Ina T, Nitani H, Abe H, Moritomo Y (2022) Coordination states of Fe³⁺ and Fe²⁺ dissolved in organic solvents. *J Physical Soc Japan* 91. <https://doi.org/10.7566/JPSJ.91.094605>
- Jiang ZY, Hunt JV, Wolff SP (1992) Ferrous ion oxidation in the presence of xylenol orange for detection of lipid hydroperoxide in low density lipoprotein. *Anal Biochem* 202:384–389. [https://doi.org/10.1016/0003-2697\(92\)90122-N](https://doi.org/10.1016/0003-2697(92)90122-N)
- Kim SE, Lee J, An JU, Kim TH, Oh CW, Ko YJ, Krishnan M, Choi J, Yoon DY, Kim Y, Oh DK (2022) Regioselectivity of an arachidonate 9S-lipoxygenase from *Sphingopyxis macrogoltabida* that biosynthesizes 9S,15S- and 11S,17S-dihydroxy fatty acids from C20 and C22 polyunsaturated fatty acids. *Biochim Biophys Acta (BBA) - Mol Cell Biol Lipids* 1867:159091. <https://doi.org/10.1016/J.BBALIP.2021.159091>
- Kim C, Eom JB, Jung S, Ji T (2016) Detection of organic compounds in water by an optical absorbance method. *Sensors (Basel)* 16. <https://doi.org/10.3390/S16010061>
- Krukowski S, Karasiewicz M, Kolodziejcki W (2017) Convenient UV-spectrophotometric determination of citrates in aqueous solutions with applications in the pharmaceutical analysis of oral electrolyte formulations. *J Food Drug Anal* 25:717–722. <https://doi.org/10.1016/J.JFDA.2017.01.009>

- Kuhn H, Gotze R, Schewe T, Rapoport SM (1981) Quasi-lipoxygenase activity of haemoglobin: a model for lipoxygenases. *Eur J Biochem* 120:161–168. <https://doi.org/10.1111/j.1432-1033.1981.tb05684.x>
- Le Guern F, Mussard V, Gaucher A, Rottman M, Prim D (2020) Fluorescein derivatives as fluorescent probes for pH monitoring along recent biological applications. *Int J Mol Sci* 21:1–23. <https://doi.org/10.3390/ijms21239217>
- Lehert N, Solomon EI (2003) Density-functional investigation on the mechanism of H-atom abstraction by lipoxygenase. *J Biol Inorg Chem* 8:294–305. <https://doi.org/10.1007/S00775-002-0415-6>
- Li Y, Schwarz PB (2018) Use of a ferrous oxidation-xylenol orange (FOX) assay to determine lipoxygenase activity in barley and malt. <https://doi-org.ezproxy.library.wur.nl/101094/ASBCJ-2012-1011-01> 70:287–289. <https://doi.org/10.1094/ASBCJ-2012-1011-01>
- Liosi GM, Dondi D, Vander Griend DA, Lazzaroni S, D'Agostino G, Mariani M (2017) Fricke-gel dosimeter: overview of xylenol orange chemical behavior. *Radiat Phys Chem* 140:74–77. <https://doi.org/10.1016/j.radphyschem.2017.01.012>
- Liu C, Liu F, Cai J, Xie UW, Long TE, Turner SR, Lyons A, Gross RA (2012) Polymers from fatty acids: poly(co-hydroxyl tetradecanoic acid) synthesis and physico-mechanical studies. *ACS Symp Ser* 1105:131–150. <https://doi.org/10.1021/BK-2012-1105.CH009>
- Lu J, Zhang C, Leong HY, Show PL, Lu F, Lu Z (2020) Overproduction of lipoxygenase from *Pseudomonas aeruginosa* in *Escherichia coli* by auto-induction expression and its application in triphenylmethane dyes degradation. *J Biosci Bioeng* 129:327–332. <https://doi.org/10.1016/j.jbiosc.2019.09.006>
- Musakhanian J, Rodier JD, Dave M (2022) Oxidative stability in lipid formulations: a review of the mechanisms, drivers, and inhibitors of oxidation. *AAPS PharmSciTech* 23. <https://doi.org/10.1208/s12249-022-02282-0>
- Mutlu H, Meier MAR (2010) Castor oil as a renewable resource for the chemical industry. *Eur J Lipid Sci Technol* 112:10–30. <https://doi.org/10.1002/EJLT.200900138>
- Newie J, Andreou A, Neumann P, Einsle O, Feussner I, Ficner R (2016) Crystal structure of a lipoxygenase from *Cyanotheca* sp. may reveal novel features for substrate acquisition. *J Lipid Res* 57:276–286. <https://doi.org/10.1194/jlr.M064980>
- Nielsen NS, Timm-Heinrich M, Jacobsen C (2003) Comparison of wet-chemical methods for determination of lipid hydroperoxides. *J Food Lipids* 10:35–50. <https://doi.org/10.1111/J.1745-4522.2003.TB00004.X>
- Pinto MDC, Tejada A, Duque AL, Macías P (2007) Determination of lipoxygenase activity in plant extracts using a modified ferrous oxidation–xylenol orange assay. *J Agric Food Chem* 55:5956–5959. <https://doi.org/10.1021/jf070537x>
- Qi Y-K, Zheng Y-C, Zhang Z-J, Xu J-H (2020) Efficient transformation of linoleic acid into 13(S)-hydroxy-9,11-(Z, E)-octadecadienoic acid using putative lipoxygenases from Cyanobacteria. *ACS Sustain Chem Eng* 8:5558–5565. <https://doi.org/10.1021/acssuschemeng.9b07457>
- Qian H, Xia B, He Y, Lu Z, Bie X, Zhao H, Zhang C, Lu F (2017) Expression, purification, and characterization of a novel acidic lipoxygenase from *Myxococcus xanthus*. *Protein Expr Purif* 138:13–17. <https://doi.org/10.1016/j.pep.2017.05.006>
- Rekowski A, Langenkämper G, Dier M, Wimmer MA, Scherf KA, Zörb C (2021) Determination of soluble wheat protein fractions using the Bradford assay. *Cereal Chem* 98:1059–1065. <https://doi.org/10.1002/cche.10447>
- Romero MV, Barrett DM (1997) Rapid methods for lipoxygenase assay in sweet corn. *J Food Sci* 62:696–700. <https://doi.org/10.1111/j.1365-2621.1997.tb15438.x>
- Sachett A, Gallas-Lopes M, Conterato GMM, Benvenuti R, Herrmann AP, Piato A (2020) Quantification of thiobarbituric acid reactive species (TBARS) optimized for zebrafish brain tissue fish behavior and physiology LAPCOM. protocols. <https://doi.org/10.17504/protocols.io.bjp8kmrw>
- Scotti M, Arosio P, Brambilla E, Gallo S, Lenardi C, Locarno S, Orsini F, Pignoli E, Pedicone L, Veronese I (2022) How xylenol orange and ferrous ammonium sulphate influence the dosimetric properties of PVA–GTA Fricke gel dosimeters: a spectrophotometric study. *Gels* 8. <https://doi.org/10.3390/gels8040204>
- Song JW, Jeon EY, Song DH, Jang HY, Bornscheuer UT, Oh DK, Park JB (2013) Multistep enzymatic synthesis of long-chain α , ω -dicarboxylic and ω -hydroxycarboxylic acids from renewable fatty acids and plant oils. *Angew Chem Int Ed* 52:2534–2537. <https://doi.org/10.1002/anie.201209187>
- Straub KL, Benz M, Schink B (2001) Iron metabolism in anoxic environments at near neutral pH. *FEMS Microbiol Ecol* 34:181–186. <https://doi.org/10.1111/j.1574-6941.2001.tb00768.x>
- Šušnovská A, Horník M, Marešová J, Pipíška M, Augustín J (2012) ¹³Cs uptake and translocation in leafy vegetable: a study with *Lactuca sativa* L. grown under hydroponic conditions. *Nova Biotechnol Et Chim* 11:153–166. <https://doi.org/10.2478/V10296-012-0018-8>
- Tadolini B, Sechi AM (1987) Iron oxidation in Mops buffer. Effect of phosphorus containing compounds. *Free Radic Res Commun* 4:161–172. <https://doi.org/10.3109/10715768709088101>
- Timabud T, Sanitchon J, Pongdontri P (2013) A modified ferrous oxidation-xylenol orange assay for lipoxygenase activity in rice grains. *Food Chem* 141:2405–2411. <https://doi.org/10.1016/j.FOODCHEM.2013.05.037>
- Vega M, Karbounea S, Husson F, Kermasha S (2005) Optimization of enzymatic assay for the measurement of lipoxygenase activity in organic solvent media. *JAOCS* 82:817–823. <https://doi.org/10.1007/s11746-005-1149-3>
- Wang Q, Liao Z, Yao D, Yang Z, Wu Y, Tang C (2021) Phosphorus immobilization in water and sediment using iron-based materials: a review. *Sci Total Environ* 767. <https://doi.org/10.1016/j.scitotenv.2020.144246>
- Waslidge NB, Hayes DJ (1995) A colorimetric method for the determination of lipoxygenase activity suitable for use in a high throughput assay format. *Anal Biochem* 231:354–358. <https://doi.org/10.1006/abio.1995.0063>
- Whent M, Ping T, Kenworthy W, Yu L (2010) High-throughput assay for detection of soybean lipoxygenase-1. *J Agric Food Chem* 58:12602–12607. <https://doi.org/10.1021/JF1028784>
- Wolff SP (1994) Ferrous ion oxidation in presence of ferric ion indicator xylenol orange for measurement of hydroperoxides. *Methods Enzymol* 233:182–189. [https://doi.org/10.1016/S0076-6879\(94\)33021-2](https://doi.org/10.1016/S0076-6879(94)33021-2)
- Yoshino T, Murakami S, Ogura K (1979) Equilibria of iron(III) complexes with xylenol orange and methylthymol blue. *J Inorg Nucl Chem* 41:1011–1013. [https://doi.org/10.1016/0022-1902\(79\)80078-0](https://doi.org/10.1016/0022-1902(79)80078-0)

Publisher's Note Springer Nature remains neutral with regard to jurisdictional claims in published maps and institutional affiliations.

Applied and Microbiology Biotechnology

A 20605

Volume 60 Number 6 February 2003

Mini-Reviews

Inagaki F, Motomura Y, Ogata S:
Microbial silica deposition in geothermal hot waters 605

Lebeau T, Robert J-M:
Diatom cultivation and biotechnologically relevant products. Part I: Cultivation at various scales 612

Lebeau T, Robert J-M:
Diatom cultivation and biotechnologically relevant products. Part II: Current and putative products 624

Gil JA, Campelo-Díez AB:
Candididin biosynthesis in *Streptomyces griseus* 633

Adachi O, Moonmangnee D, Toyama H, Yamada M, Shinagawa E, Matsushita K:
New developments in oxidative fermentation 643

Shokri A, Sandén AM, Larsson G:
Cell and process design for targeting of recombinant protein into the culture medium of *Escherichia coli* 654

Yoshida K, Koethien P, Matsui T, Kawaoka A, Shimmyo A:
Molecular biology and application of plant peroxidase genes 665

Biotechnological products and process engineering

Roble ND, Ogbonna JC, Tanaka H:
A novel circulating loop bioreactor with cells immobilized in loofa (*Luffa cylindrica*) sponge for the bioconversion of raw cassava starch to ethanol 671

Hild HM, Stuckey DC, Leak DJ:

Effect of nutrient limitation on product formation during continuous fermentation of xylose with *Thermoanaerobacter ethanolicus* JW200 (Fet3) 679

Toh SK, Tay JH, Moy BYP, Ivanov V, Tay STL:
Size-effect on the physical characteristics of the aerobic granule in a SBR 687

Haq I, Ali S, Qadeer MA, Iqbal J:
Inductive effect of cresoquinone on microbiological transformation of L-tyrosine to 3,4 dihydroxy phenyl L-alanine by *Aspergillus oryzae* NG-11^{PS} (Short contribution) 696

Biotechnologically relevant enzymes and proteins

Xiao YZ, Tu XM, Wang J, Zhang M, Cheung Q, Zeng WY, Shi YY:
Purification, molecular characterization and reactivity with aromatic compounds of a laccase from basidiomycete *Trametes* sp. strain AH28-2 700

Pilz R, Hammer E, Schauer F, Kragl U:
Laccase-catalysed synthesis of coupling products of phenolic substrates in different reactors (Short contribution) 708

(Continued on inside front cover)



Springer

Online First
Immediately Online
<http://link.springer.de>
<http://link.springer-ny.com>

Faster publication!



Applied Microbiology and Biotechnology

Publishing model: Open access

[← Back to Overview](#)

Editors

Editor-in-Chief

Professor Dr. rer. nat. Alexander Steinbüchel, Department of Molecular Microbiology and Biotechnology, University of Münster, Germany

Managing Editor

Dr. rer. nat. Dorothea Kessler, Schriesheim, Germany

Associate Editors

Julio César Carrero Sánchez, PhD, Department of Immunology, Instituto de Investigaciones Biomedicas, Universidad Nacional Autonoma de Mexico, Mexico City, Mexico

Hermann J. Heipieper, PhD, Helmholtz Centre for Environmental Research, UFZ Leipzig, Germany

Professor Dr. rer. nat. Ursula Kües, Georg-August-Universität Göttingen, Buisgeninstitut, Abteilung Molekulare Holzbiotechnologie und Technische

Mykologie, Göttingen, Germany

Professor Bing Li, PhD, Institute of Environment and Ecology,
Tsinghua Shenzhen International Graduate School, Tsinghua University,
Shenzhen, China

Professor Xueting Liu, PhD, State Key Laboratory of Bioreactor Engineering, East
China University of Science and Technology, Shanghai, China

Professor Thomas Mansell, PhD, Chemical & Biological Engineering, Iowa State
University, Ames, United States

Professor Sergio Sanchez, MD, PhD, Instituto de Investigaciones Biomédicas,
Universidad Nacional Autónoma de México, Mexico

Professor Kunihiro Watanabe, PhD, Division of Applied Life Sciences, Graduate
School of Life and Environmental Sciences, Kyoto Prefectural University, Japan

Professor Lixin Zhang, PhD, State Key Laboratory of Bioreactor Engineering,
East China University of Science and Technology, Shanghai, China

Editors

Professor Hal Alper, PhD, McKetta Department of Engineering, Cockrell School of
Engineering, University of Austin, Texas, United States

Professor George N. Bennett, PhD, Department of Biochemistry & Cell Biology,
Rice University, Houston, Texas, United States

Professor Uwe T. Bornscheuer, PhD, Department of Biotechnology & Enzyme
Catalysis, Institute of Biochemistry, University of Greifswald, Germany

Professor Dr. rer. nat. Axel A. Brakhage, Department of Molecular and Applied
Microbiology, Hans-Knöll-Institute Jena, Germany

Professor Dr. sc. nat. Gerhard H. Braus, Department of Microbiology and
Genetics, Institute of Molecular Microbiology and Genetics, Georg-August
University Göttingen, Germany

George Guo-qiang Chen, PhD, Department of Biology, Tsinghua University,
Beijing, China

Professor Douglas J. Cork, PhD, Department of Biological and Chemical Sciences,

Illinois Institute of Technology, Chicago, Illinois, United States

Professor Uwe Deppenmeier, PhD, Institut für Mikrobiologie und Biotechnologie, Rheinische Friedrich-Wilhelms-Universität Bonn, Germany

Gerrit Eggink, PhD, Food and Biobased Research and AlgaePARC, Wageningen University and Research, Wageningen, The Netherlands

Professor Shinya Fushinobu, PhD, Department of Biotechnology, The University of Tokyo, Japan

Navdeep Grover, PhD, Heparin Applied Research Center, Rensselaer Polytechnic Institute, Troy, New York, USA

Bruce K. Hamilton, PhD, U.S. National Science Foundation (NSF), Arlington, Virginia, United States

Professor Yoshiteru Hashimoto, MD, Graduate School of Life and Environmental Sciences, University of Tsukuba, Tsukuba, Japan

Professor emeritus Michael Hecker, PhD, Microbial Physiology and Molecular Biology, University of Greifswald, Germany

Soon-Kwang Hong, PhD, Division of Bioscience and Bioinformatics, Myongji University, Yongin, Republic of Korea

Masayuki Inui, PhD, Research Institute of Innovative Technology for the Earth RITE, Kyoto, Japan

Nemat O. Keyhani, PhD, Department of Biological Sciences, University of Illinois, United States

Professor Tasuo Kurihara, PhD, Institute for Chemical Research, Kyoto, Japan

Professor Sang Yup Lee, PhD, Department of Chemical and Biomolecular Engineering, Korea Advanced Institute of Science and Technology, Daejeon, Korea

Z. Lewis Liu, PhD, USDA-ARS National Center for Agricultural Utilization Research, Peoria, United States

Xiangyang Liu, PhD, Department of Biological Sciences, UW-Milwaukee, Milwaukee, Wisconsin, United States

Professor José M. Luengo, PhD, Department of Molecular Biology, University of León, Spain

- Professor Dr. rer. nat. techn. Diethard Mattanovich**, Department of Biotechnology, University of Natural Resources and Life Sciences, Vienna, Austria
- Professor Ian Menz, PhD**, School of Life Sciences, University of Technology Sydney (UTS), Australia
- Professor Hisaaki Mihara, PhD**, Ritsumeikan University, Kyoto, Japan
- Professor Jörg Nickelsen, PhD**, Ludwig-Maximilians-Universität, Munich, Germany
- Professor Jens Nielsen, PhD**, Chalmers University of Technology, Gothenburg, Sweden
- Professor Kevin O'Connor, PhD**, School of Biomolecular and Biomedical Science, Science Centre, University College Dublin, Ireland
- Masayuki Okuyama, PhD**, Division of Applied Bioscience, Research Faculty of Agriculture, Hokkaido University, Sapporo, Japan
- Professor E. Terry Papoutsakis, PhD**, Delaware Biotechnology Institute, University of Delaware, Newark, Delaware, United States
- Professor Pamela Peralta-Yahya, PhD**, School of Chemistry & Biochemistry, College of Sciences, Georgia Tech, Atlanta, Georgia, United States
- Professor Bernd H.A. Rehm, PhD**, Centre for Cell Factories and Biopolymers, Griffith Institute for Drug Discovery, Nathan, Queensland, Australia
- Badal C. Saha, PhD**, Agricultural Research Service, United States Department of Agriculture, Peoria, Illinois, United States
- Carmen Sanchez, PhD**, Department of Biotechnology, Universidad Autónoma de Tlaxcala, Mexico
- Professor Dr. rer. nat. Thomas H. Scheper**, Institute of Technical Chemistry, Leibniz University Hannover, Germany
- Frank-Rainer Schmidt, PhD**, Sanofi-Aventis Deutschland, Prozessentwicklung Chemie, Industriepark Höchst, Frankfurt am Main, Germany
- Professor Helmut Schwab, PhD**, Department of Molecular Biotechnology, Technical University Graz, Austria
- Yasushi Shigeri, PhD**, Department of Chemistry, Wakayama Medical University,

Wakayama, Japan

Professor Anthony J. Sinskey, Sc.D., Massachusetts Institute of Technology, Cambridge, Massachusetts, United States

Daniel K.Y. Solaiman, PhD, Eastern Regional Research Center, Agricultural Research Service, United States Department of Agriculture, Wyndmoor, Pennsylvania, United States

Professor A.J.J. Straathof, PhD, Department of Biotechnology, Delft University of Technology, The Netherlands

Professor Kenji Ueda, PhD, Life Science Research Center, College of Bioresource Sciences, Nihon University, Kanagawa, Japan

Professor Dr. rer. nat. Roland Ulber, Department of Mechanical and Process Engineering, Institute of Bioprocess Engineering, Technical University Kaiserslautern, Germany

Professor Mark C.M. van Loosdrecht, PhD, Department of Biotechnology, Delft University of Technology, The Netherlands

Professor Volker F. Wendisch, PhD, Genetics of Prokaryotes, Faculty of Biology & CeBiTec, Bielefeld University, Germany

Professor Paul J. Weimer, PhD, Department of Bacteriology, University of Wisconsin, Madison, USA

Professor Dr. rer. nat. Josef Winter, Institute of Bioengineering and Biotechnology of Wastewater, Karlsruhe Institute of Technology (KIT), Germany

Shotaro Yamaguchi, PhD, Medical Enzymes Division, Amano Enzyme Inc., Nagoya, Japan

Professor Yeo Joon Yoon, PhD, College of Pharmacy, Seoul National University, South Korea

Professor Takeshi Zendo, PhD, Department of Bioscience and Biotechnology, Faculty of Agriculture, Kyushu University, Fukuoka, Japan

Professor Tong Zhang, PhD, Environmental Microbiome Engineering and Biotechnology Lab, Department of Civil Engineering, University of Hong Kong, *Hong Kong SAR, China*



Applied Microbiology and Biotechnology

Publishing model: Open access

[← Back to Overview](#)

[Search all Applied Microbiology and Biotechnology articles →](#)

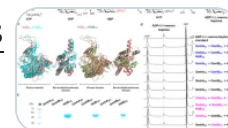


Volume 108, Issue 1

December 2024

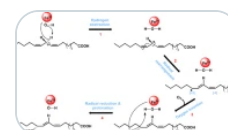
267 articles in this issue

Characterization of the ADP- β -d-manno-heptose biosynthetic enzymes from two pathogenic *Vibrio* strains

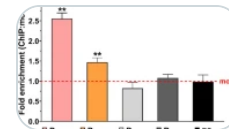


Biotechnologically Relevant Enzymes and Proteins | Open access | 18 March 2024 | Article: 267

Versatile ferrous oxidation-xylene orange assay for high-throughput screening of lipoxygenase activity

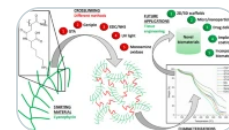


Unveiling the repressive mechanism of a PPS-like regulator (PspR) in polyhydroxyalkanoates biosynthesis network



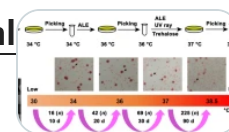
Applied Microbial and Cell Physiology | Open access | 18 March 2024 | Article: 265

Cyanophycin modifications for applications in tissue scaffolding



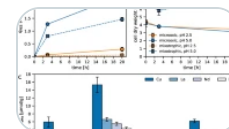
Biotechnological Products and Process Engineering | Open access | 15 March 2024 | Article: 264

Adaptive responses of erythritol-producing *Yarrowia lipolytica* to thermal stress after evolution



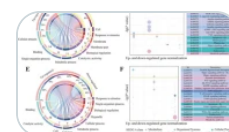
Genomics, Transcriptomics, Proteomics | Open access | 15 March 2024 | Article: 263

Roles of pH and phosphate in rare earth element biosorption with living acidophilic microalgae



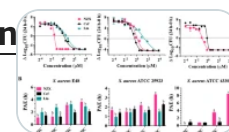
Environmental Biotechnology | Open access | 14 March 2024 | Article: 262

Dynamics and regulatory role of circRNAs in Asian honey bee larvae following fungal infection



Genomics, Transcriptomics, Proteomics | Open access | 13 March 2024 | Article: 261

Pharmacokinetics and pharmacodynamics of antibacterial peptide NZX in *Staphylococcus aureus* mastitis mouse model



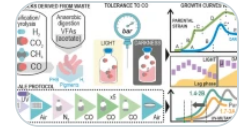
Biotechnologically Relevant Enzymes and Proteins | Open access | 13 March 2024 | Article: 260

Computational aptamer design for spike glycoprotein (S) (SARS CoV-2) detection with an electrochemical aptasensor



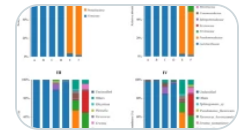
Methods and Protocols | Open access | 12 March 2024 | Article: 259

Exploring *Rhodospirillum rubrum* response to high doses of carbon monoxide under light and dark conditions



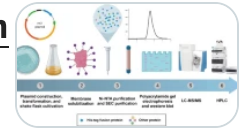
Applied Microbial and Cell Physiology | Open access | 11 March 2024 | Article: 258

Effects of inoculation and dry matter content on microbiome dynamics and metabolome profiling of sorghum silage



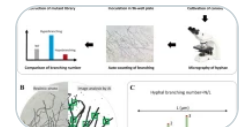
Applied Microbial and Cell Physiology | Open access | 08 March 2024 | Article: 257

Expression, purification, and characterization of transmembrane protein homogentisate solanesyltransferase



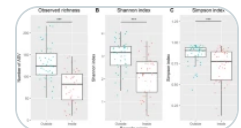
Biotechnologically Relevant Enzymes and Proteins | Open access | 07 March 2024 | Article: 256

The serine/threonine protein kinase MpSTE1 directly governs hyphal branching in *Monascus* spp.



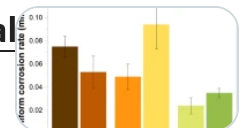
Applied Microbial and Cell Physiology | Open access | 06 March 2024 | Article: 255

Identifying environmental factors affecting the microbial community composition on outdoor structural timber



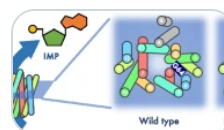
Environmental Biotechnology | Open access | 06 March 2024 | Article: 254

Synergistic corrosion effects of magnetite and microorganisms: microbial community dependency



Black yeasts in hypersaline conditions

Mini-Review | Open access | 05 March 2024 | Article: 252

Mutational analysis in *Corynebacterium stationis* MFS transporters for improving nucleotide bioproduction

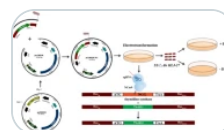
Biotechnologically Relevant Enzymes and Proteins | Open access | 04 March 2024 | Article: 251

Acremonium sp. diglycosidase-aid chemical diversification: valorization of industry by-products

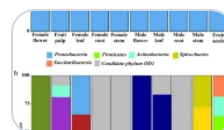
Biotechnologically Relevant Enzymes and Proteins | Open access | 02 March 2024 | Article: 250

X-ray structure and characterization of a probiotic *Lactobacillus rhamnosus* Probio-M9 L-rhamnose isomerase

Biotechnologically Relevant Enzymes and Proteins | Open access | 02 March 2024 | Article: 249

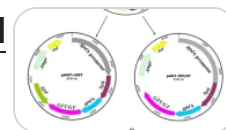
Assessing immunogenicity of CRISPR-NCas9 engineered strain against porcine epidemic diarrhea virus

Applied Genetics and Molecular Biotechnology | Open access | 02 March 2024 | Article: 248

Unraveling endophytic diversity in dioecious *Siraitia grosvenorii*: implications for mogroside production

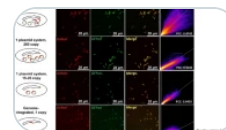
Applied Microbial and Cell Physiology | Open access | 01 March 2024 | Article: 247

A newly discovered glycosyltransferase gene *UGT88A1* affects growth and polysaccharide synthesis of *Grifola frondosa*



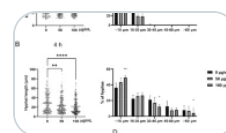
Applied Genetics and Molecular Biotechnology | Open access | 29 February 2024 | Article: 246

The non-mevalonate pathway requires a delicate balance of intermediates to maximize terpene production



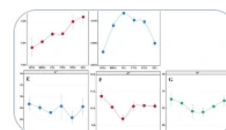
Applied Genetics and Molecular Biotechnology | Open access | 29 February 2024 | Article: 245

Secretory IgA reduced the ergosterol contents of *Candida albicans* to repress its hyphal growth and virulence



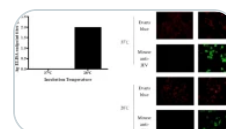
Applied Microbial and Cell Physiology | Open access | 29 February 2024 | Article: 244

Analyzing microbial community and volatile compound profiles in the fermentation of cigar tobacco leaves



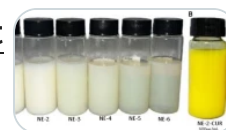
Biotechnological Products and Process Engineering | Open access | 29 February 2024 | Article: 243

Low-temperature culture enhances production of flavivirus virus-like particles in mammalian cells



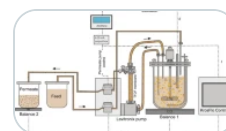
Biotechnological Products and Process Engineering | Open access | 28 February 2024 | Article: 242

Olive oil nanoemulsion containing curcumin: antimicrobial agent against multidrug-resistant bacteria



Biotechnological Products and Process Engineering | Open access | 27 February 2024 | Article: 241

Production of recombinant vesicular stomatitis virus-based vectors by tangential flow depth filtration

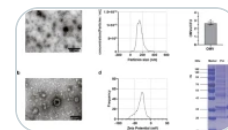


A type III polyketide synthase cluster in the phylum *Planctomycetota* is involved in alkylresorcinol biosynthesis



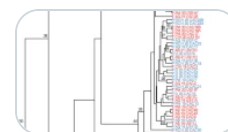
Applied Genetics and Molecular Biotechnology | Open access | 26 February 2024 | Article: 239

Characterization and immunological effect of outer membrane vesicles from *Pasteurella multocida* on macrophages



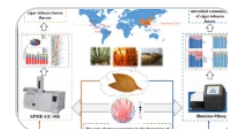
Applied Microbial and Cell Physiology | Open access | 26 February 2024 | Article: 238

Genetic structure and population diversity of *Phytophthora infestans* strains in Pacific western Canada



Applied Genetics and Molecular Biotechnology | Open access | 26 February 2024 | Article: 237

Correlation study on microbial communities and volatile flavor compounds in cigar tobacco leaves of diverse origins



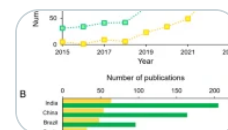
Applied Microbial and Cell Physiology | Open access | 26 February 2024 | Article: 236

Recent advance of microbial mercury methylation in the environment



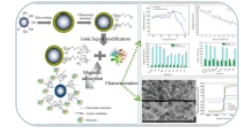
Mini-Review | Open access | 26 February 2024 | Article: 235

Tailor-made solvents for microbial carotenoids recovery



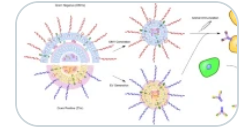
Mini-Review | Open access | 24 February 2024 | Article: 234

Characterization of a recombinant *Aspergillus niger* GZUF36 lipase immobilized by ionic liquid modification strategy



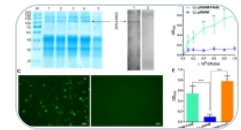
Biotechnologically Relevant Enzymes and Proteins | Open access | 24 February 2024 | Article: 233

Outer membrane vesicles as a platform for the discovery of antibodies to bacterial pathogens



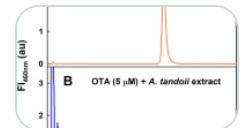
Mini-Review | Open access | 24 February 2024 | Article: 232

An M cell-targeting recombinant *L. lactis* vaccine against four *H. pylori* adhesins



Biotechnological Products and Process Engineering | Open access | 23 February 2024 | Article: 231

A new and promiscuous α/β hydrolase from *Acinetobacter tandoii* DSM 14970^T inactivates the mycotoxin ochratoxin A



Biotechnologically Relevant Enzymes and Proteins | Open access | 23 February 2024 | Article: 230



Part of 1 collection:

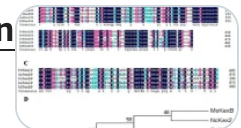
Food security and sustainability from a microbiology perspective

Construction of viral-based expression vectors for high-level production of human interferon alpha 2b in plants



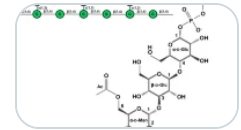
Biotechnologically Relevant Enzymes and Proteins | Open access | 23 February 2024 | Article: 229

FvKex2 is required for development, virulence, and mycotoxin production in *Fusarium verticillioides*



Applied Microbial and Cell Physiology | Open access | 22 February 2024 | Article: 228

Xanthan: enzymatic degradation and novel perspectives of applications



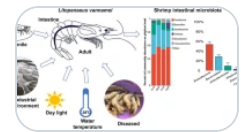
Mini-Review | Open access | 21 February 2024 | Article: 227

The microbial biosynthesis of noncanonical terpenoids



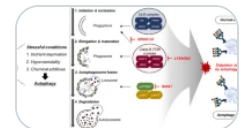
Mini-Review | Open access | 21 February 2024 | Article: 226

Profile of the gut microbiota of Pacific white shrimp under industrial indoor farming system



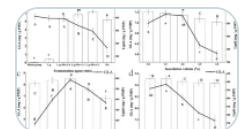
Applied Microbial and Cell Physiology | Open access | 20 February 2024 | Article: 225

Effects of autophagy-inhibiting chemicals on sialylation of Fc-fusion glycoprotein in recombinant CHO cells



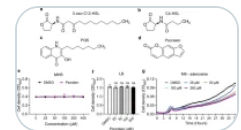
Biotechnological Products and Process Engineering | Open access | 20 February 2024 | Article: 224

Production of polyunsaturated fatty acids in pork backfat fermented by *Mucor circinelloides*



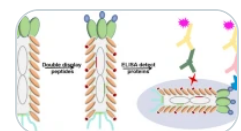
Biotechnological Products and Process Engineering | Open access | 20 February 2024 | Article: 223

Discovery of psoralen as a quorum sensing inhibitor suppresses *Pseudomonas aeruginosa* virulence

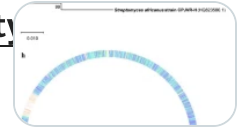


Applied Microbial and Cell Physiology | Open access | 19 February 2024 | Article: 222

Advanced detection of cervical cancer biomarkers using engineered filamentous phage nanofibers

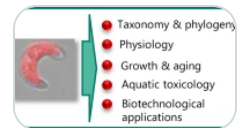


[Streptomyces enissocaesilis L-82 has broad-spectrum antibacterial activity and promotes growth for *Carassius auratus*](#)



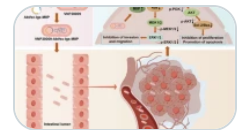
Environmental Biotechnology | Open access | 19 February 2024 | Article: 220

[Features of the microalga *Raphidocelis subcapitata*: physiology and applications](#)



Mini-Review | Open access | 19 February 2024 | Article: 219

[VNP20009-Abvec-Igk-MIIP suppresses ovarian cancer progression by modulating Ras/MEK/ERK signaling pathway](#)



Applied Microbial and Cell Physiology | Open access | 19 February 2024 | Article: 218

1 2 ... 6 Next >

For authors

[Submission guidelines](#) →

[Language editing services](#) ↗

[Ethics and disclosures](#) →

[How to publish with us](#)



[Fees and funding](#)



[Contact the journal](#)



[Collections and calls for papers](#)



Language quality checker

[Get your manuscript edited for free](#) →

[Use our pre-submission checklist](#) →

Avoid common mistakes on your manuscript.



[This journal's calls for papers →](#)

Collections this journal is participating in.



[Sign up for alerts →](#)

Get notified when new articles are published.



Explore

[Articles](#)



[Volumes and issues](#)



[Collections](#)





Ads by Google

Stop seeing this ad Why this ad?

Applied Microbiology and Biotechnology

COUNTRY

Germany



Universities and research institutions in Germany



Media Ranking in Germany

SUBJECT AREA AND CATEGORY

Biochemistry, Genetics and Molecular Biology
Biotechnology

Immunology and Microbiology
Applied Microbiology and Biotechnology

Medicine
Medicine (miscellaneous)

PUBLISHER

Springer Verlag

H-INDEX

253

PUBLICATION TYPE

Journals

ISSN

14320614,
01757598

COVERAGE

1984-2022

INFORMATION

[Homepage](#)



[How to publish in this journal](#)

AMBoffice@gmx.de

SCOPE

Mini-Reviews are short reviews critically summarizing the current state of and providing perspectives on biotechnological processes, products, microbial genomes, methods and equipment. Papers should deal with the following aspects of applied microbiology and biotechnology: Biotechnological products and process engineering Established and in pipe technologies of biotechnological processes using prokaryotic or eukaryotic cells or enzymes and other proteins for production, conversion, degradation and detection of substances including bioreactor design. Biotechnologically relevant enzymes and proteins Characterization of hitherto undescribed, biotechnologically relevant enzymes and proteins or of known proteins with novel properties and purification of proteins on a technical scale. Bioenergy and biofuels Biotechnological processes for production of fuels, combustible chemicals and other forms of energy. Applied genetics and molecular biotechnology New vectors and methods for genetic transformation and all aspects of strain improvement employing recombinant DNA technology including metabolic engineering and enzyme engineering. Genomics, transcriptomics, proteomics Characterization and analyses of genomes, transcriptomes and proteomes. Applied microbial and cell physiology Physiological studies on biosynthesis, catabolism and biotransformation of biotechnologically relevant compounds. Environmental biotechnology All aspects of environmental processes using microorganisms and biodegradation of hazardous chemicals. Methods and protocols Novel methods and techniques or significant modifications of already described methods or new combinations of methods yielding significant improvements. Their novelty and reliability must be concisely presented.

 Join the conversation about this journal

 Quartiles


←

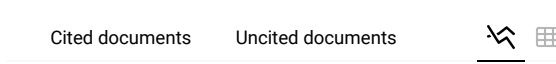
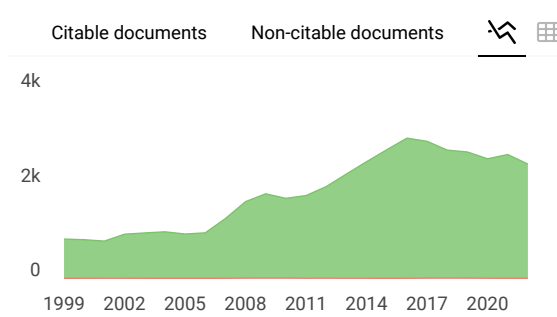
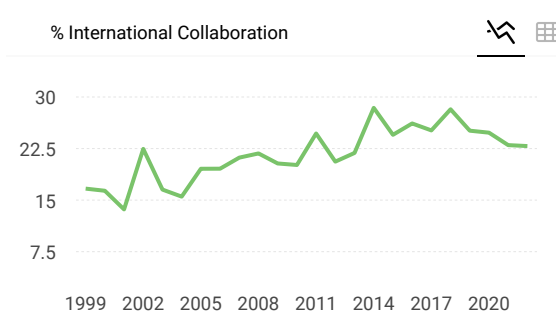
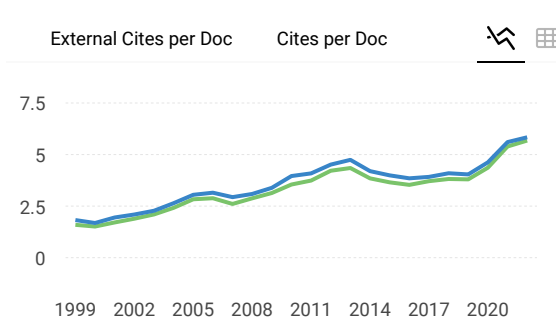
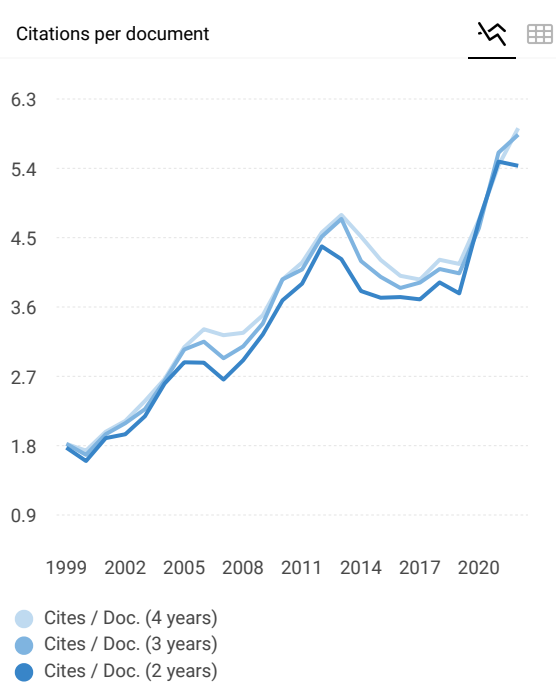
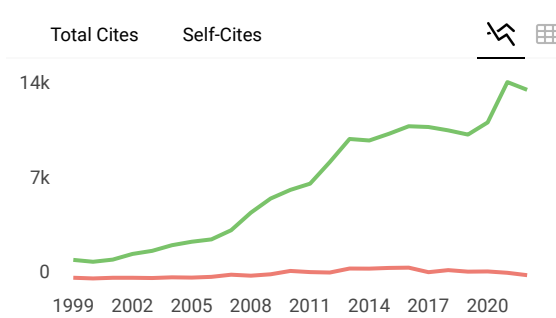
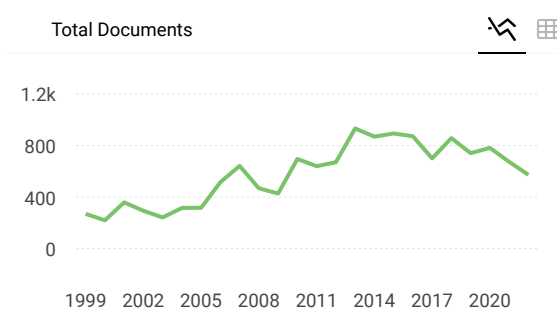
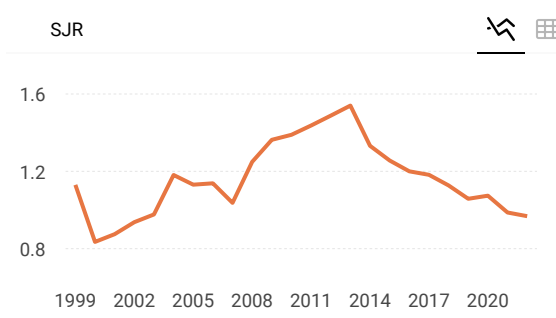
Ads by Google

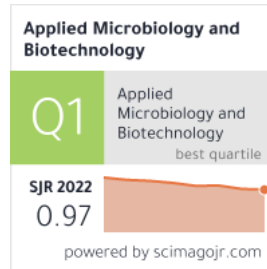
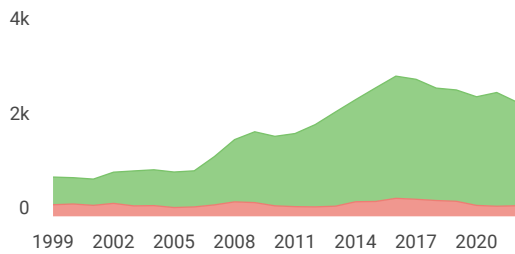
Stop seeing this ad

Why this ad? 

FIND SIMILAR JOURNALS ?

<p>1 AMB Express</p> <p>DEU</p> <p>93% similarity</p>	<p>2 World Journal of Microbiology and</p> <p>NLD</p> <p>84% similarity</p>	<p>3 Microbial Biotechnology</p> <p>GBR</p> <p>81% similarity</p>	<p>4 Microbial Cell Fa</p> <p>GBR</p> <p>79' similarity</p>
---	---	---	---





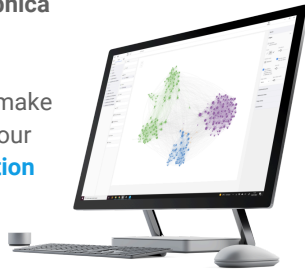
← Show this widget in your own website

Just copy the code below and paste within your html code:

```
<a href="https://www.scimagojr.com" data-bbox="614 145 754 159">
```

SCImago Graphica

Explore, visually communicate and make sense of data with our [new data visualization tool](#).



Metrics based on Scopus® data as of April 2023

V **Veronica** 1 year ago

what it is the impact factor of this journal according to SJR ?

reply



Melanie Ortiz 1 year ago

SCImago Team

Dear Veronica, thank you very much for your comment. SCImago Journal and Country Rank uses Scopus data, our impact indicator is the SJR. We suggest you consult the Journal Citation Report for other indicators (like Impact Factor) with a Web of Science data source. Best Regards, SCImago Team

A **A.E.Z. Hasan** 3 years ago

I will submit articles to your journal. Hopefully, the article will finish soon. best regards...aez hasan (biochemistry, IPB University)

reply



Melanie Ortiz 3 years ago

Dear Hasan, thanks for your participation! Best Regards, SCImago Team

V Vinitha Pai 3 years ago

Hello; Good morning. We have done a study - the isolation purification and characterization of a phytochemical which has anti-Pseudomonas activity against Pseudomonas aeruginosa isolated from used industrial coolant- Will this be appropriate for your journal ?

We have also standardised the procedure for using the extract in coolant to extend the life of the coolant which is the basis for an Indian patent application. Do we have a chance of publishing this in your esteemed journal.

reply



Melanie Ortiz 3 years ago

Dear Vinitha,

thank you for contacting us.

We are sorry to tell you that SCImago Journal & Country Rank is not a journal. SJR is a portal with scientometric indicators of journals indexed in Elsevier/Scopus.

Unfortunately, we cannot help you with your request, we suggest you visit the journal's homepage (See scope and submission/author guidelines) or contact the journal's editorial staff , so they could inform you more deeply.

Best Regards, SCImago Team

D Dudha Raj Malla Thakuri 3 years ago

i want to published artical

reply



Melanie Ortiz 3 years ago

Dear Dudha, thank you very much for your comment, we suggest you look for author's instructions/submission guidelines in the journal's website. Best Regards, SCImago Team

Leave a comment

Name

Email

(will not be published)



Source details

Applied Microbiology and Biotechnology

Formerly known as: European Journal of Applied Microbiology and Biotechnology

Scopus coverage years: from 1984 to Present

Publisher: Springer Nature

ISSN: 0175-7598 E-ISSN: 1432-0614

Subject area: Immunology and Microbiology: Applied Microbiology and Biotechnology

Biochemistry, Genetics and Molecular Biology: Biotechnology

Source type: Journal

CiteScore 2022

9.9



SJR 2022

0.968



SNIP 2022

1.275



[View all documents >](#)

[Set document alert](#)

[Save to source list](#)

[CiteScore](#) [CiteScore rank & trend](#) [Scopus content coverage](#)

CiteScore 2022

$$9.9 = \frac{26.764 \text{ Citations 2019 - 2022}}{2.703 \text{ Documents 2019 - 2022}}$$

Calculated on 05 May, 2023

CiteScoreTracker 2023

$$10.0 = \frac{24.378 \text{ Citations to date}}{2.439 \text{ Documents to date}}$$

Last updated on 05 March, 2024 • Updated monthly

CiteScore rank 2022

Category	Rank	Percentile
Immunology and Microbiology	#16/121	87th
Applied Microbiology and Biotechnology		
Biochemistry, Genetics and Molecular Biology	#45/299	85th
Biotechnology		

[View CiteScore methodology >](#) [CiteScore FAQ >](#) [Add CiteScore to your site &](#)

About Scopus

[What is Scopus](#)

[Content coverage](#)

[Scopus blog](#)

[Scopus API](#)

[Privacy matters](#)

Language

[日本語版を表示する](#)

[查看简体中文版本](#)

[查看繁體中文版本](#)

[Просмотр версии на русском языке](#)

Customer Service

[Help](#)

[Tutorials](#)

[Contact us](#)

ELSEVIER

[Terms and conditions](#) ↗ [Privacy policy](#) ↗

All content on this site: Copyright © 2024 Elsevier B.V. ↗, its licensors, and contributors. All rights are reserved, including those for text and data mining, AI training, and similar technologies. For all open access content, the Creative Commons licensing terms apply.

We use cookies to help provide and enhance our service and tailor content. By continuing, you agree to the use of cookies ↗.



Saya bukan robot
reCAPTCHA
Privasi · Persyaratan

Submit

The users of Scimago Journal & Country Rank have the possibility to dialogue through comments linked to a specific journal. The purpose is to have a forum in which general doubts about the processes of publication in the journal, experiences and other issues derived from the publication of papers are resolved. For topics on particular articles, maintain the dialogue through the usual channels with your editor.

Developed by:



Powered by:



Follow us on @ScimagoJR

Scimago Lab, Copyright 2007-2022. Data Source: Scopus®

EST MODUS IN REBUS
Horatio (Satire 1, 1, 106)

[Legal Notice](#)

[Privacy Policy](#)